Journal of Mathematical Biology manuscript No.
(will be inserted by the editor)

Structured Models of Cell Migration Incorporating Molecular Binding Processes

Pia Domschke · Dumitru Trucu · Alf Gerisch · Mark A. J. Chaplain

Received: date / Accepted: date

Abstract The dynamic interplay between collective cell movement and the various molecules involved in the accompanying cell signalling mechanisms plays a crucial role in many biological processes including normal tissue development and pathological scenarios such as wound healing and cancer. Information about the various structures embedded within these processes allows a detailed exploration of the binding of molecular species to cell-surface receptors within the evolving cell population. In this paper we establish a general *spatio-temporal-structural* framework that enables the description of molecular binding to cell membranes coupled with the cell population dynamics. We first provide a general theoretical description for this approach and then illustrate it with three examples arising from cancer invasion.

Keywords structured population model · spatio-temporal model · cell-surface receptors · cancer invasion

Pia Domschke · Alf Gerisch
Fachbereich Mathematik, Technische Universität Darmstadt
Dolivostr. 15, 64293 Darmstadt, Germany
E-mail: domschke@mathematik.tu-darmstadt.de
E-mail: gerisch@mathematik.tu-darmstadt.de

Dumitru Trucu
Division of Mathematics, University of Dundee
Dundee DD1 4HN, United Kingdom
E-mail: trucu@maths.dundee.ac.uk

Mark A. J. Chaplain
School of Mathematics and Statistics, Mathematical Institute, University of St Andrews
St Andrews KY16 9SS, United Kingdom
E-mail: majc@st-andrews.ac.uk

1 Introduction

The modelling of complex biological systems has witnessed extensive developments over the past four decades. Ranging from studying large-scale collective behaviour of inter-linked species in ecological studies to the understanding of the complicated multiscale processes arising in animal and human cell and tissue biology, the modelling has gradually evolved in scope and focus to include not only temporal and spatial coordinates but also structural information of the individual species involved, such as age, size or other relevant quantifiable aspects (Förste, 1978; Metz and Diekmann, 1986).

Spatio-temporal models, in particular reaction-diffusion-taxis systems, have a long history not only in mathematical biology research (Skellam, 1951) but in the wider applied mathematics community. Such modelling approaches have generally avoided incorporating any structural information in them (e.g. age, size). The development of structured-population models also has a long tradition going back to the seminal work of von Foerster (1959). Areas of interest for structured-population modelling include ecology, epidemiology, collective cell movement in normal tissue dynamics and pathological situations, such as malignant solid tumours and leukaemia, to name a few. A majority of these models have been concerned with coupling time and structure (e.g. age, size) in individual or collective species dynamics (Trucco, 1965a,b; Sinko and Streifer, 1967; Gyllenberg, 1982; Diekmann et al, 1984; Kunisch et al, 1985; Gyllenberg, 1986; Gyllenberg and Webb, 1987; Tucker and Zimmerman, 1988; Diekmann et al, 1992; Diekmann and Metz, 1994; Huyer, 1994; Calsina and Saldaña, 1995; de Roos, 1997; Cushing, 1998; Basse and Ubezio, 2007; Chapman et al, 2007). Models coupling space and structure were also developed (Gurtin and MacCamy, 1981; MacCamy, 1981; Förste, 1978; Garroni and Langlais, 1982; Huang, 1994; Rhandi, 1998; Langlais and Milner, 2003; Ayati, 2006; Delgado et al, 2006; Allen, 2009), and these have paved the way towards modelling approaches that couple time, space, and structure, opening a new era in the modelling of biological processes (Di Blasio, 1979; Busenberg and Iannelli, 1983; Langlais, 1988; Fitzgibbon et al, 1995; Rhandi and Schnaubelt, 1999; So et al, 2001; Al-Omari and Gourley, 2002; Cusulin et al, 2005; Deng and Hallam, 2006).

Central to the study of structured population models, is the role played by the semigroup framework (Webb, 1985; Metz and Diekmann, 1986; Gyllenberg and Webb, 1990; Diekmann et al, 1992). Approaches based on delay-differential equations explore the behaviour of the system under consideration in the presence of age, size, or various other appropriate structural information (Mackey and Glass, 1977; Angulo et al, 2012). Questions regarding the spatio-structural controllability in single species population models have also been addressed by Gyllenberg (1983); Ainseba and Langlais (2000); Ainseba and Anita (2001); Gyllenberg et al (2002). Discrete spatial or temporal and continuous in structure models have been equally employed to understand various ecological processes (Gyllenberg et al, 1997; Gyllenberg and Hanski, 1997; Matter et al, 2002; de Camino-Beck and Lewis, 2009; Lewis et al, 2010). These

methodologies have been recently complemented with novel measure theory approaches such as the ones proposed by Gwiazda and Marciniak-Czochra (2010). Finally, numerical explorations and computational simulations have also become increasingly present within the range of methods for the analysis of temporal-structural, spatio-structural, and *spatio-temporal-structural* models (Ayati, 2000; Ayati et al, 2006; Ayati and Dupont, 2002; Abia et al, 2009).

Of recent interest is the exploration of structural information within the context of modelling the complex links between cell movement and the cascade of signalling pathway mechanisms appearing within diseases like cancer, both in malignant solid tumours (Basse et al, 2003, 2004, 2005; Basse and Ubezio, 2007; Ayati et al, 2006; Daukste et al, 2012; Gabriel et al, 2012) and leukaemia (Bernard et al, 2003; Foley and Mackey, 2009; Roeder et al, 2009), as well as in hematopoietic diseases such as autoimmune hemolytic anemia (Bélair et al, 1995; Mahaffy et al, 1998).

Although much progress has been made through *in vivo* and *in vitro* research, understanding more deeply the cross-talk between signalling molecules and the individual and collective cell dynamics in human tissue remains a major challenge for the scientific community. The development of a suitable theoretical framework coupling dynamics at the cell population level with dynamics at the level of cell-surface receptors and molecules is crucial in understanding many important normal and pathological cellular processes. To this end, despite all the experimental advancements, mathematical modelling coupling cell-scale structural information with spatial and temporal dynamics is still in its very early days, with only a few recent works on the subject such as those proposing an age-structured spatio-temporal haptotaxis modelling in tumour progression (Walker, 2007, 2008, 2009) as well as those addressing the link between age structure and cell cycle and proliferation (Gabriel et al, 2012; Billy et al, 2014) or exploring the role of membrane inhomogeneities for individual cells' deformation mechanics (Mercker et al, 2013). However, none of these modelling attempts have addressed so far the mutual coupling between the collective cell movement and the binding behaviour of the different molecules which are part of the various molecular signalling pathways that may come under consideration in the overall tissue dynamics.

The importance of accounting for molecular binding in addressing the overall tissue dynamics is well illustrated and necessary in the case of cancer invasion. In order to be able to degrade the extracellular matrix (ECM), cancer cells require cell-surface bound matrix metalloproteinase that are referred to as MT1-MMP (Rowe and Weiss, 2009; Sabeh et al, 2009). In this situation, among the secreted matrix metalloproteinases (MMP), only the bound MT1-MMP become active through binding to the cancer cell membrane. In this way the cancer cells acquire the ability to alter the ECM constituents. However, the rest of MMP molecules that are unbound (either due to unbinding or because they do not bind to cancer cell membranes) are not able to degrade the ECM, and hence do not contribute directly to cancer invasion. We highlight this in Section 3.1 where we consider a simple situation when just a single

type of MMP molecules are being expressed by the cancer cells. The ability to account explicitly for binding in model (33) provides clear benefits over the usual reaction-diffusion-taxis spatio-temporal model (27) which cannot distinguish between bound and unbound MMP sub-populations. These are explored numerically later in the same section and show significant differences in the ECM degradation rate and overall cancer invasion speed.

In this contribution we focus on the binding (and unbinding) of molecules to (and from) the cell surface which gives rise to variations of the surface concentration of these surface-bound molecules. Thus, for a particular molecular species, we distinguish the free (unbound) concentration and, if binding to the cell surface takes place, the surface concentration. The free concentration is typically subject to molecular diffusion and is represented as a dependent (on time and space) variable in our modelling framework. In contrast to that, the surface concentration is not subject to independent molecular diffusion as surface-bound molecules travel along with the cell they are bound to. We accommodate this *travelling along* in our modelling framework by representing the surface concentration of such a molecule as a so-called structural variable, a further independent variable in addition to time and space, of the cell density. The goal of this work is to address the coupling between the collective cell dynamics and the cell surface binding behaviour of different types of accompanying molecules. This is achieved by establishing the fundamentals of a general framework that captures the overall coupled interaction of a *spatio-temporal-structural* cell population density accompanied by a number of binding spatio-temporal molecular species concentrations. This explores the binding, activation and inhibition processes between cell surface-bound and free molecular species and their effect on the overall cell-population dynamics.

The paper is structured as follows. In Section 2 we introduce the modelling framework by deriving, from the first principle, a general spatio-temporal-structural model which can take cell surface binding processes of different kind into account. From this, we will derive a corresponding non-structured model by integrating over the structure space. Section 3 is devoted to the application of this novel spatio-temporal-structural modelling framework to derive three specific structured models that describe (part of) the cancer cell invasion process. We demonstrate numerically the influence of the structure in these models and compare to existing models from the literature. Finally, in Section 4 we discuss the new framework and give insights for further developments.

2 A Spatio-Temporal-Structural Modelling Framework

In this section we establish a general framework for our spatio-temporal-structural population model that enables the coupling of cell surface-bound reaction processes with the overall cell population dynamics.

Let $\mathcal{D} \subset \mathbb{R}^d$, $d \in \{1, 2, 3\}$, be a bounded spatial domain, $\mathcal{I} = (0, T]$, $0 < T \in \mathbb{R}$, be the time interval, and $\mathcal{P} \subset \mathbb{R}^p$, $p \in \mathbb{N}$, be a convex domain of admissible structure states that contains $\mathbf{0} \in \mathbb{R}^p$ as accumulation point. The set $\mathcal{P}$ will

be referred to as the i-state space (Metz and Diekmann, 1986) (= *individual's state*). Here the temporal, spatial, and structural variables are t, x, and y, respectively. Our basic model consists of the following dependent variables:

- the structured cell density $c(t, x, y)$, with $(t, x, y) \in \mathcal{I} \times \mathcal{D} \times \mathcal{P}$;
- the extracellular matrix (ECM) density $v(t, x)$, with $(t, x) \in \mathcal{I} \times \mathcal{D}$;
- q free molecular species, of concentration $m_i(t, x)$, with $(t, x) \in \mathcal{I} \times \mathcal{D}$, $i = 1, \ldots, q$, which may be written in vector notation

$$\mathbf{m} = (m_1, \ldots, m_q)^{\mathsf{T}} : \mathcal{I} \times \mathcal{D} \to \mathbb{R}^q \,.$$

We consider that p of the free molecular species are able to bind to the surface of the cells; without loss of generality, these are m_i, $i = 1, \ldots, p$, with $p \leq q$. Note that the number p of molecular species being able to bind to a cell's surface corresponds to the dimension of the i-state space $\mathcal{P}$. Similar to size-structured population models, see for example Chapman et al (2007); Diekmann et al (1984) or Tucker and Zimmerman (1988), we model the surface concentration of bound molecules on the surface of the cells by the structure or i-state variable $y \in \mathcal{P}$. This gives rise to the structured cell density $c(t, x, y)$, which denotes the cell number density at a time t of cells at a spatial point x that have a surface concentration equal to y of molecules bound to their surface. Hence, the unit of $c(t, x, y)$ is number of cells per unit volume in space (at x) per unit volume in the i-state (at y). The surface concentrations y_i, $i = 1, \ldots, p$, are measured in [µmol/cm^2], which yields a unit volume in the p-dimensional i-state y of [(µmol/cm^2)^p] and thus the unit of the structured cell density c is given by [cells/(cm^3 · (µmol/cm^2)^p)].

The total, that is non-structured, cell density C at t and x is then obtained by integrating the structured cell density over all i-states $y \in \mathcal{P}$,

$$C(t, x) = \int_{\mathcal{P}} c(t, x, y) \, \mathrm{d}y \,, \tag{1}$$

and its unit is therefore given in [cells/cm^3].

The *structured cell surface density* $s(t, x, y)$, in contrast to the above structured cell *number* density, gives, per unit volume in space and per unit volume in the i-state, the surface area of those cells at t and x which have surface concentration y. Let us assume that all cells have the same fixed cell surface area ε with unit [cm^2/cell]. Then the structured cell surface density can be expressed as

$$s(t, x, y) = \varepsilon c(t, x, y) \tag{2}$$

and has unit [cm^2/(cm^3 · (µmol/cm^2)^p)].

The representation of binding and unbinding events in our modelling framework requires that we are able to convert between the surface concentration of a bound molecular species and a corresponding concentration per unit volume in space of this bound molecular species. To this end, we denote by $\mathbf{n}(t, x)$ the

bound molecular species volume concentration at given t and x. Multiplication of the structured cell surface density $s(t,x,y)$ with the respective surface concentration y yields the *structured volume concentration* of the bound molecular species per unit volume in the i-state. Thus, integration of this structured volume concentration over the i-state space $\mathcal{P}$ yields the desired bound molecular species volume concentration, i.e.,

$$\mathbf{n}(t,x) = (n_1(t,x),\dots,n_p(t,x))^\mathsf{T} := \int_{\mathcal{P}} ys(t,x,y)\,\mathrm{d}y \quad \in \mathbb{R}^p\,. \tag{3}$$

The unit of n_i, $i = 1,\dots,p$, is [µmol/cm^3] = [nM], which is the same as the unit for the *free molecular species volume concentrations* m_j, $j = 1,\dots,q$.

Finally, by the density of the ECM we refer to the *mass density of the fibrous proteins inside the ECM*, for example collagen, hence the unit of the ECM density is [mg/cm^3].

For a compact notation, we define the combined vector of the structured cell density and the ECM density as well as the combined vector of bound and free molecular species volume concentrations by

$$\mathbf{u}(t,x) := \begin{pmatrix} c(t,x,\cdot) \\ v(t,x) \end{pmatrix} : \mathcal{P} \to \mathbb{R}^2 \quad \text{and} \quad \mathbf{r}(t,x) := \begin{pmatrix} \mathbf{n}(t,x) \\ \mathbf{m}(t,x) \end{pmatrix} \in \mathbb{R}^{p+q}\,, \tag{4}$$

respectively.

Since some of the processes modelled are limited due to spatial constraints, we define the *volume fraction of occupied space* by

$$\hat{\rho}(t,x) \equiv \rho(C(t,x), v(t,x)) := \vartheta_c C(t,x) + \vartheta_v v(t,x) \tag{5}$$

with suitable parameters ϑ_c and ϑ_v. Note that with this definition we assume the amount of free and bound molecular species to be negligible for the volume fraction of occupied space.

With these preparatory definitions and considerations in place, we now derive and discuss the model equations for the evolution of c, v and $\mathbf{m}$ in Sections 2.1, 2.2, and 2.3, respectively.

Remark 1 The quantities defined above can be interpreted in a measure-theoretic framework and so can terms in the equations presented in the following subsections. For example, the bound molecular species volume concentrations $\mathbf{n}(t,x)$, see Eq. (3), can be seen as an expected value and the definition of the binding and unbinding rates in the structural flux, see the discussion in the end of Section 2.1 below, becomes more general in such a context. We refer the interested reader to Appendix A, where we elucidate these issues in some detail.

2.1 Cell population

Consider, inside the *spatio-structural* space $\mathcal{D}\times\mathcal{P}$, an arbitrary control volume $V\times W$, satisfying that V and W are compact with piecewise smooth boundaries ∂V and ∂W. The total amount of cells in $V \times W$ at time t is

$$C_{V\times W}(t) = \int_W \int_V c(t,x,y)\,\mathrm{d}x\,\mathrm{d}y\,.$$

Per unit time, the rate of change in $C_{V\times W}$ is given by the combined effect of the sources of cells of the structural types considered over the control volume and the flux of cells into the control volume over the spatial and structural boundaries. Therefore, we have the integral form of the balance law given by

$$\begin{aligned}\frac{dC_{V\times W}}{dt} = &\underbrace{\int_W \int_V S(t,x,y)\,\mathrm{d}x\,\mathrm{d}y}_{\text{source}} - \underbrace{\int_W \int_{\partial V} F(t,x,y)\cdot\mathfrak{n}(x)\,\mathrm{d}\sigma_{n-1}(x)\,\mathrm{d}y}_{\text{flux over spatial boundary}}\\ &\underbrace{-\int_V \int_{\partial W} G(t,x,y)\cdot\mathfrak{n}(y)\,\mathrm{d}\sigma_{p-1}(y)\,\mathrm{d}x}_{\text{flux over structural boundary}}\,,\end{aligned} \tag{6}$$

where σ_{n-1} and σ_{p-1} are the surface measures on ∂V and ∂W, respectively. Assuming that the vector fields F and G are continuously differentiable and since V and W are compact with piecewise smooth boundaries, the divergence theorem yields

$$\begin{aligned}\frac{dC_{V\times W}}{dt} = &\int_W \int_V S(t,x,y)\,\mathrm{d}x\,\mathrm{d}y - \int_W \int_V \nabla_x\cdot F(t,x,y)\,\mathrm{d}x\,\mathrm{d}y\\ &- \int_V \int_W \nabla_y\cdot G(t,x,y)\,\mathrm{d}y\,\mathrm{d}x\,.\end{aligned} \tag{7}$$

Assuming further that c and c_t are continuous, Leibniz's rule for differentiation under the integral sign (Halmos, 1978) gives

$$\begin{aligned}\int_W \int_V \frac{\partial}{\partial t}c(t,x,y)\,\mathrm{d}x\,\mathrm{d}y = &\int_W \int_V S(t,x,y)\,\mathrm{d}x\,\mathrm{d}y - \int_W \int_V \nabla_x\cdot F(t,x,y)\,\mathrm{d}x\,\mathrm{d}y\\ &- \int_W \int_V \nabla_y\cdot G(t,x,y)\,\mathrm{d}x\,\mathrm{d}y\,.\end{aligned} \tag{8}$$

Since this holds for arbitrary control volumes $V \times W$, we obtain the following partial differential equation, i.e. the corresponding differential form of the balance law for the structured cell density:

$$\frac{\partial}{\partial t}c(t,x,y) = S(t,x,y) - \nabla_x\cdot F(t,x,y) - \nabla_y\cdot G(t,x,y)\,. \tag{9}$$

This form is similar to models of velocity-jump processes, where the i-state describes the velocity and potentially other internal states of an individual, see, for example, Othmer et al (1988); Erban and Othmer (2005); Xue et al (2009, 2011); Kelkel and Surulescu (2012); Othmer and Xue (2013); Engwer et al (2015); Xue (2015).

Source. The source of the cell population is given by the proliferation of the cells through cell division (there may be other cell sources, even negative ones such as apoptosis, but here we only consider cell division). Let $\Phi(y, \mathbf{u})$ be the rate at which cells undergo mitosis (proliferation rate). Similar to equal mitosis in size-structured populations as was considered by Perthame (2007), we assume that, as cells divide, the daughter cells share the p different molecular species on their surface equally. That means that a cell at (t, x, y) divides into two cells at $(t, x, \frac{1}{2}y)$, and a schematic of this can be seen in Figure 1.

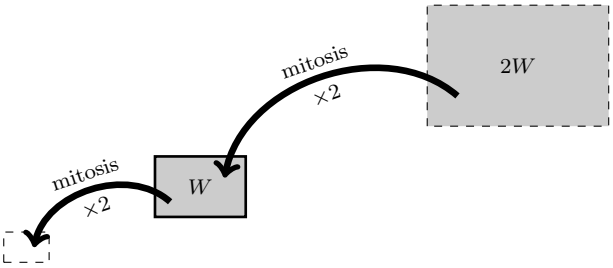

Figure 1: Individuals leaving and entering the control volume $W \subset \mathcal{P}$ through mitosis.

As was done in Metz and Diekmann (1986), we impose the following

Convention 1 *If a transformed i-state argument falls outside $\mathcal{P}$ we shall assume that the term in which it occurs equals zero.*

Then, for an arbitrary control volume $W \subset \mathcal{P}$, the source of cells in W is given by

$$\int_W S(t,x,y)\,\mathrm{d}y = 2\int_{2W} \Phi(\tilde{y}, \mathbf{u}(t,x,\tilde{y}))c(t,x,\tilde{y})\,\mathrm{d}\tilde{y} - \int_W \Phi(y, \mathbf{u}(t,x,y))c(t,x,y)\,\mathrm{d}y\,. \tag{10}$$

Equation (10) is obvious if W, $2W$, and $\frac{1}{2}W$ are pairwise disjoint. For the general case with arbitrary W we refer to the proof in Appendix B. For the integral over $2W$, we use the change of variables $\tilde{y}(y) = 2y$, for which $\det(J_{\tilde{y}}) = 2^p$, and obtain

$$\begin{aligned}&\int_W S(t,x,y)\,\mathrm{d}y\\ =&\int_W 2^{p+1}\Phi(2y, \mathbf{u}(t,x,2y))c(t,x,2y)\,\mathrm{d}y - \int_W \Phi(y, \mathbf{u}(t,x,y))c(t,x,y)\,\mathrm{d}y\,.\end{aligned}$$

Since this holds for any control volume W, we get

$$S(t,x,y) = 2^{p+1}\Phi(2y, \mathbf{u}(t,x,2y))c(t,x,2y) - \Phi(y, \mathbf{u}(t,x,y))c(t,x,y)\,, \forall y \in \mathcal{P}. \tag{11}$$

Spatial flux. The flux over the spatial boundary results from a combination of diffusion (random motion), chemotaxis (with respect to various free molecular species volume concentrations), and haptotaxis (with respect to the ECM density) of the structured cell population. Here we define the diffusion and taxis terms following Andasari et al (2011); Gerisch and Chaplain (2008) as

$$F(t,x,y) = -D_c\nabla_x c + c(1-\rho(C,v))\left(\sum_{k=1}^{q}\chi_k\nabla_x m_k + \chi_v\nabla_x v\right), \tag{12}$$

where the free molecular species with volume concentration m_k may either act as chemoattractants ($\chi_k > 0$) or as chemorepellents ($\chi_k < 0$). We assume that the diffusion coefficient $D_c(\cdot)$ as well as the taxis coefficients $\chi_v(\cdot)$ and $\chi_k(\cdot)$, $k = 1,\ldots,q$, can, in particular, depend on the i-state $y \in \mathcal{P}$. More complex forms of (12) are indeed conceivable and we provide an initial discussion in Section 4.

Structural flux. The flux over the structural boundary represents changes in the i-state, that is changes in the surface concentration of bound molecules on the cells' surface, and thus results from binding and unbinding events of molecules to and from the cells' surface.

We assume that the binding rates of the free molecular species $m_1, ..., m_p$ to the cell surface depend on the already bound molecules on the cell surface, i.e. the i-state y, as well as on the available free molecules, i.e. the free molecular species volume concentration $\mathbf{m}(t,x)$. Thus we denote the non-negative binding rate vector by $\mathbf{b}(y,\mathbf{m}) \in \mathbb{R}^p$. In contrast, we assume that the unbinding rates only depend on the i-state y, which implies that unbinding is not restricted by $\mathbf{m}(t,x)$. Thus we denote the non-negative unbinding rate vector by $\mathbf{d}(y) \in \mathbb{R}^p$. In summary, these binding and unbinding rates lead to an associated *net binding rate* for the i-state y given by $\mathbf{b}(y,\mathbf{m}) - \mathbf{d}(y)$. The net binding rate describes an amount of molecules bound per surface area per unit time, hence the unit of this rate is given by $[(\mu\text{mol}/\text{cm}^2)/\text{s}]$.

Since the i-state space $\mathcal{P}$ is defined as the set of all admissible structure states, it is necessary that the net binding rate vector field does not point out of $\mathcal{P}$ on $\partial\mathcal{P}$, i.e. that

$$(\mathbf{b}(y,\mathbf{m}) - \mathbf{d}(y))\,\mathfrak{n}(y) \le 0 \qquad \text{for } t \in \mathcal{I}\,,\ x \in \overline{\mathcal{D}}\,,\ y \in \partial\mathcal{P}\,, \tag{13}$$

where $\mathfrak{n}(y)$ denotes the outer unit normal vector on $\partial\mathcal{P}$ in $y \in \partial\mathcal{P}$. This condition must be fulfilled by the particular choice of $\mathbf{b}$ and $\mathbf{d}$ in specific models.

Now the flux is given by the product of the structured cell density and the net binding rate, hence has the form

$$G(t,x,y) = c(t,x,y)\big(\mathbf{b}(y,\mathbf{m}) - \mathbf{d}(y)\big)\,. \tag{14}$$

This form maintains the interpretation of the structural flux $G(t,x,y)$ as, for example, growth in size-structured populations (Chapman et al, 2007; Tucker and Zimmerman, 1988; Metz and Diekmann, 1986; Webb, 2008).

2.2 Extracellular matrix

The extracellular matrix (ECM) consists of fibrous proteins such as collagen or vitronectin. These proteins are assumed to be static, i.e. we do not consider any transport terms for the ECM. The ECM is degraded by one or more of the free molecular species or the surface-bound reactants and is remodelled by the stroma cells present in the tissue (which are not modelled explicitly). The equation for the ECM is then

$$\frac{\partial}{\partial t}v(t,x) = -\underbrace{\boldsymbol{\delta}_v^{\mathsf{T}}\mathbf{r}(t,x)v(t,x)}_{\text{degradation}} + \underbrace{\psi_v(t,\mathbf{u}(t,x))}_{\text{remodelling}}\,,$$

where $\boldsymbol{\delta}_v \in \mathbb{R}^{p+q}$ is the non-negative vector of ECM degradation rates and $\psi_v(t,\mathbf{u})$ represents the remodelling term. To ensure non-negativity of the ECM density, we require $\psi_v(t,\mathbf{u}) \geq 0$ for $v = 0$. A common formulation for the remodelling term is a constant rate together with a volume-filling term, see, e.g., Domschke et al (2014),

$$\psi_v(t,\mathbf{u}(t,x)) = \mu_v(1 - \rho(C(t,x), v(t,x)))^+\,, \tag{15}$$

where $(\cdot)^+ := \max\{0,\cdot\}$.

2.3 Molecular species

We assume that the free molecular species, as described by their volume concentrations m_i, $i = 1,\dots,q$, rearrange spatially driven by diffusion only. Furthermore, they are produced by either the cells directly or by chemical reactions. Potentially, some of the species undergo natural decay. The first p species may also bind to and unbind from the cell surface. All these effects can be captured in the following equation describing the dynamics of all free molecular species volume concentrations:

$$\begin{aligned}\frac{\partial}{\partial t}\mathbf{m}(t,x) = \underbrace{\nabla_x\cdot[\mathbf{D}_\mathbf{m}\nabla_x\mathbf{m}(t,x)]}_{\text{diffusion}} - \underbrace{\int_{\mathcal{P}}\Big(\hat{\mathbf{b}}(y,\mathbf{m}) - \hat{\mathbf{d}}(y)\Big)\,s(t,x,y)\,\mathrm{d}y}_{\text{binding/unbinding}} \\ + \underbrace{\boldsymbol{\psi}_\mathbf{m}(\mathbf{u}(t,x),\mathbf{r}(t,x))}_{\text{production}} - \underbrace{\operatorname{diag}(\boldsymbol{\delta}_\mathbf{m})\mathbf{m}(t,x)}_{\text{decay}}\,.\end{aligned} \tag{16}$$

In the above, $\mathbf{D_m} = \mathrm{diag}(D_{m_1}, \ldots, D_{m_q}) \in \mathbb{R}^{q,q}$ denotes the diagonal matrix containing the non-negative diffusion constants of the individual species. Furthermore, $\boldsymbol{\psi}_\mathbf{m}(\mathbf{u}, \mathbf{r})$ is the vector of production terms, which depends on the structured cell and ECM densities and the free as well as bound molecular species volume concentrations. This production term is in particular i-state-dependent, explicitly through c and implicitly through $\mathbf{n}$, and thus provides influence of the structure on the dynamics of the overall system. This is a strong feature of our structured modelling framework and the necessity of such a feature provided the main initial motivation to consider a structured approach. The modelling examples in Section 3 will highlight this in more detail. In order to ensure the non-negativity of $\mathbf{m}$, we require, for $j = 1, \ldots, q$, that $(\boldsymbol{\psi}_\mathbf{m}(\mathbf{u}, \mathbf{r}))_j \geq 0$ if $m_j = 0$. Next, the vector $\boldsymbol{\delta}_\mathbf{m}$ contains the non-negative rates of decay of the individual species. Finally, we discuss the reasoning behind the remaining binding/unbinding term in more detail below.

The rate of change of $\mathbf{m}$ due to binding or unbinding events to the cell surface is zero for the components $p+1, p+2, \ldots, q$ since those do not bind to the cell surface. Thus we will derive the appropriate rate of change for the first p components below. For a unified treatment of all components, however, we extend the binding and unbinding rate vectors by zeros, that is we define

$$\hat{\mathbf{b}}(y, \mathbf{m}) = \begin{pmatrix} \mathbf{b}(y, \mathbf{m}) \\ \mathbf{0} \end{pmatrix} \in \mathbb{R}^q \quad \text{and} \quad \hat{\mathbf{d}}(y) = \begin{pmatrix} \mathbf{d}(y) \\ \mathbf{0} \end{pmatrix} \in \mathbb{R}^q \,. \tag{17}$$

The rate of change of the volume concentration $\mathbf{m}$ due to binding or unbinding events to cell surfaces is the combined effect of the corresponding rates of change per i-state; thus the binding/unbinding term in (16) is an integral over the i-state space. The rate of change of the volume concentration $\mathbf{m}$ due to binding/unbinding to/from cell surfaces in i-state y can be seen as the product of the net binding rate $\hat{\mathbf{b}}(y, \mathbf{m}) - \hat{\mathbf{d}}(y)$, which gives the amount of molecules being bound per surface area per unit time ($[(\mu\mathrm{mol}/\mathrm{cm}^2)/\mathrm{s}]$), and the structured cell surface density $s(t, x, y)$, which denotes, per unit volume in space and per unit volume in the i-state, the surface area of the cells at t and x that have surface concentration y ($[\mathrm{cm}^2/(\mathrm{cm}^3 \cdot (\mu\mathrm{mol}/\mathrm{cm}^2)^p)]$). This explains the integrand in the binding/unbinding term in (16). Furthermore note that a positive component j of the net binding rate means that the volume concentration m_j decreases and thus the minus sign in front of the integral is required. Finally, observe that the earlier conditions on the binding rate vector $\mathbf{b}$ ensure non-negativity of $\mathbf{m}$.

2.4 Summary of the model, non-dimensionalisation, initial and boundary conditions

For the convenience of the reader, we summarise below the equations of the structured model for the structured cell density, the ECM density, and the

free molecular species volume concentrations as they have been derived in Sections 2.1, 2.2, and 2.3, respectively:

$$\begin{aligned}\frac{\partial c}{\partial t} &= \nabla_x \cdot \left[D_c \nabla_x c - c(1-\rho(C,v)) \left(\sum_{k=1}^{q} \chi_k \nabla_x m_k + \chi_v \nabla_x v \right) \right] \\ &\quad - \nabla_y \cdot \left[(\mathbf{b}(y,\mathbf{m}) - \mathbf{d}(y))\, c \right] \\ &\quad + 2^{p+1} \Phi(2y, \mathbf{u}(t,x,2y)) c(t,x,2y) - \Phi(y, \mathbf{u}(t,x,y)) c(t,x,y)\,,\end{aligned} \tag{18a}$$

$$\frac{\partial v}{\partial t} = -\boldsymbol{\delta}_v^{\mathsf{T}} \mathbf{r} v + \psi_v(t, \mathbf{u})\,, \tag{18b}$$

$$\begin{aligned}\frac{\partial \mathbf{m}}{\partial t} &= \nabla_x \cdot [\mathbf{D}_\mathbf{m} \nabla_x \mathbf{m}] - \int_{\mathcal{P}} \left(\hat{\mathbf{b}}(y,\mathbf{m}) - \hat{\mathbf{d}}(y) \right) s \,\mathrm{d}y \\ &\quad + \boldsymbol{\psi}_\mathbf{m}(\mathbf{u}, \mathbf{r}) - \mathrm{diag}(\boldsymbol{\delta}_\mathbf{m}) \mathbf{m}\,.\end{aligned} \tag{18c}$$

In the above, we have suppressed the arguments (t,x) and (t,x,y) except in the proliferation term in Eq. (18a) where it is necessary to show its dependence on $2y$.

We non-dimensionalise system (18) by using the following dimensionless quantities

$$\begin{gathered}\tilde{t} = \frac{t}{\tau}, \qquad \tilde{x} = \frac{x}{L}, \qquad \tilde{y} = \frac{y}{y_*}, \\ \tilde{c}(\tilde{t},\tilde{x},\tilde{y}) = \frac{c(t,x,y)}{c_*}, \quad \tilde{v}(\tilde{t},\tilde{x}) = \frac{v(t,x)}{v_*}, \quad \tilde{\mathbf{m}}(\tilde{t},\tilde{x}) = \frac{\mathbf{m}(t,x)}{m_*}.\end{gathered} \tag{19}$$

The scaling parameters are given in Appendix C and the appropriate non-dimensionalised model parameters are collected there in Table 1. The units and non-dimensionalisation of intermediate quantities are shown in Table 2. With the scalings defined in (19), the system obtained by non-dimensionalisation of (18) looks identical to the original one, but with a tilde on each quantity. For notational convenience we will omit the tilde signs in the following but will consider system (18) as the non-dimensionalised system and always refer to non-dimensionalised quantities. For the convenience of the reader, we state here that the non-dimensional form of the volume fraction of occupied space, cf. (5), takes, for non-dimensional $C(t,x)$ and $v(t,x)$, the form

$$\rho(C(t,x), v(t,x)) = C(t,x) + v(t,x)\,. \tag{20}$$

System (18) is supposed to hold for $t \in \mathcal{I}$, $x \in \mathcal{D}$ and $y \in \mathcal{P}$ and is completed by initial conditions

$$c(0,x,y) = c_0(x,y)\,, \quad v(0,x) = v_0(x)\,, \quad \mathbf{m}(0,x) = \mathbf{m}_0(x) \quad \text{for } x \in \overline{\mathcal{D}}, y \in \overline{\mathcal{P}}\,, \tag{21}$$

and zero-flux boundary conditions in space, that is

$$\begin{aligned}\left[D_c\nabla_x c - c(1-\rho(C,v))\left(\sum_{k=1}^{q}\chi_k\nabla_x m_k + \chi_v\nabla_x v\right)\right]\cdot\mathfrak{n}(x) = 0\,,\\ [\mathbf{D_m}\nabla_x\mathbf{m}]\cdot\mathfrak{n}(x) = \mathbf{0}\,,\\ \text{for } t\in\mathcal{I}\,,\ x\in\partial\mathcal{D}\,,\ y\in\overline{\mathcal{P}}\,,\end{aligned} \tag{22}$$

where $\mathfrak{n}(x)$ denotes the unit outer normal vector on $\partial\mathcal{D}$ in $x\in\partial\mathcal{D}$.

Since the equation for the structured cell density (18a) is hyperbolic in the i-state variable, we can only impose boundary conditions on the inflow boundary part of $\mathcal{P}$, i.e., where $[\mathbf{b}(y,\mathbf{m})-\mathbf{d}(y)]\cdot\mathfrak{n}(y)<0$ holds. Here, $\mathfrak{n}(y)$ denotes the unit outer normal vector on $\partial\mathcal{P}$ in $y\in\partial\mathcal{P}$. Clearly, the inflow boundary part of $\mathcal{P}$ may change with (t,x) through changes in $\mathbf{m}(t,x)$ and is thus denoted and defined by

$$\partial\mathcal{P}_{in}(t,x) := \{y\in\partial\mathcal{P} : [\mathbf{b}(y,\mathbf{m}(t,x))-\mathbf{d}(y)]\cdot\mathfrak{n}(y)<0\}\ . \tag{23}$$

Since we assume that no cells with i-states outside $\mathcal{P}$ exist, we impose a zero Dirichlet boundary condition on the inflow boundary of the i-state space, that is

$$c(t,x,y) = 0 \qquad \text{for } t\in\mathcal{I}, x\in\overline{\mathcal{D}}, y\in\partial\mathcal{P}_{in}(t,x)\,. \tag{24}$$

Recall that, according to our modelling, cells in i-state $y\in\mathcal{P}$ divide into cells in i-state $y/2\in\mathcal{P}$ since $\mathcal{P}$ is convex with accumulation point 0. Thus the proliferation term in the structured cell density equation does not create cells on the boundary of $\mathcal{P}$ and is thus consistent with the above zero Dirichlet boundary condition on $\partial\mathcal{P}_{in}(t,x)$.

On the part of $\partial\mathcal{P}$, where we do not have an inflow situation, i.e. where we cannot prescribe boundary conditions, the flux in outer normal direction is zero, which follows directly from (13). On the inflow boundary $\partial\mathcal{P}_{in}$, where we impose zero Dirichlet boundary conditions, the flux in outer normal direction is also zero and hence, for the whole boundary of the i-state space $\mathcal{P}$ it holds that

$$[(\mathbf{b}(y,\mathbf{m})-\mathbf{d}(y))\,c]\,\mathfrak{n}(y) = 0 \qquad \text{for } t\in\mathcal{I}\,,\ x\in\overline{\mathcal{D}}\,,\ y\in\partial\mathcal{P}\,. \tag{25}$$

We provide a more detailed discussion of these boundary conditions in the presentation of the specific models in Section 3.

2.5 Derivation of a non-structured model corresponding to (18)

The total cell density $C(t,x)$ is obtained by integrating the structured cell density $c(t,x,y)$ over the i-state-space $\mathcal{P}$. The aim of this section is to take the structured model (18) as a starting point and to derive a suitable, corresponding non-structured model. That model will be formulated exclusively in

terms of the non-structured quantities $C(t,x)$, $v(t,x)$, and $\mathbf{m}(t,x)$. Please note that $v(t,x)$, and $\mathbf{m}(t,x)$ in the non-structured model will not be identical with the variables of the same name in the structured model because their defining equations will be different since structured terms need to be approximated by non-structured ones. However, their principle meaning will be the same and thus we chose to also stick with the same variable names.

In the derivation of the non-structured model below it is necessary to approximate terms involving structured expressions with expressions which involve only variables of the non-structured model. For our purposes here, this will be achieved, in general, by replacing structured terms by their i-state mean as well as the structured cell density by its mean value with respect to the i-state space; higher-order approximations of the latter are of course possible and we comment on these in the conclusion in Section 4. In order to proceed, we first define the mean structured cell density and the centre of mass of the i-state space $\mathcal{P}$ by,

$$\bar{c}(t,x) := \frac{1}{|\mathcal{P}|}\int_{\mathcal{P}} c(t,x,y)\,\mathrm{d}y = \frac{1}{|\mathcal{P}|}C(t,x) \quad \text{and} \quad \bar{y} = \frac{1}{|\mathcal{P}|}\int_{\mathcal{P}} y\,\mathrm{d}y\,,$$

respectively.

The parameters $D_c(y)$, $\chi_k(y)$ for $k = 1,\ldots,1$, and $\chi_v(y)$ of the spatial flux expression (12) are replaced by their mean values over the i-state space. These constants are denoted by $\bar{D}_c$, $\bar{\chi}_k$, and $\bar{\chi}_v$, respectively. Also, the (extended) binding and unbinding rate vectors, $\hat{\mathbf{b}}(y,\mathbf{m})$ and $\hat{\mathbf{d}}(y)$, respectively, see (17), are replaced by their i-state-means, which are denoted by $\overline{\hat{\mathbf{b}}}(\mathbf{m})$ and $\overline{\hat{\mathbf{d}}}$, respectively.

The situation is different and more involved in, for example, the bound molecular species volume concentrations $\mathbf{n}$, since its defining expression depends on the i-state y explicitly but also implicitly through the structured cell density $c(t,x,y)$. In this case we replace $c(t,x,y)$ by its i-state mean $\bar{c}(t,x)$ and obtain the following approximation

$$\mathbf{n}(t,x) = \int_{\mathcal{P}} y\varepsilon c(t,x,y)\,\mathrm{d}y \approx \varepsilon C(t,x)\frac{1}{|\mathcal{P}|}\int_{\mathcal{P}} y\,\mathrm{d}y = \varepsilon\bar{y}C(t,x) =: \bar{\mathbf{n}}(t,x)\,.$$

The new quantity $\bar{\mathbf{n}}(t,x)$ is computable from non-structured quantities and can thus be used in the non-structured model. We are now in the position to introduce the following non-structured versions of $\mathbf{u}$ and $\mathbf{r}$

$$\bar{\mathbf{u}}(t,x) := \begin{pmatrix}\bar{c}(t,x)\\ v(t,x)\end{pmatrix} \quad \text{and} \quad \bar{\mathbf{r}}(t,x) := \begin{pmatrix}\bar{\mathbf{n}}(t,x)\\ \mathbf{m}(t,x)\end{pmatrix}\,.$$

We can now further approximate the proliferation rate $\Phi(y,\mathbf{u})$ as follows

$$\Phi(y,\mathbf{u}) \approx \Phi(y,\bar{\mathbf{u}}) \approx \bar{\Phi}(\bar{\mathbf{u}})\,,$$

where the first approximation is the replacement of $c(t,x,y)$ by $\bar{c}(t,x)$ and the second approximation (which might be exact) is the determination of the

i-state mean of $\Phi(y, \bar{\mathbf{u}})$. In a similar fashion we arrive at the approximation $\bar{\psi}_v(t, \bar{\mathbf{u}})$ for the remodelling term $\psi_v(t, \mathbf{u})$ in the ECM density equation (18b) and at the approximation $\bar{\boldsymbol{\psi}}_{\mathbf{m}}(\bar{\mathbf{u}}, \bar{\mathbf{r}})$ for the production term $\boldsymbol{\psi}_{\mathbf{m}}(\mathbf{u}, \mathbf{r})$ in the free molecular species volume concentration equation (18c).

With all the above preparatory definitions and approximations at hand, we now derive the non-structured model and start by integrating the structured cell density, i.e. Eq. (18a), over the i-state space. Under the assumption that we can exchange integration and differentiation on the left-hand side, i.e. that we can apply Leibniz's rule for differentiation under the integral sign (Halmos, 1978), we obtain

$$\begin{aligned}\frac{\partial C}{\partial t} =& \int_{\mathcal{P}} \left(\nabla_x \cdot \left[D_c \nabla_x c - c(1-\rho(C,v)) \left(\sum_{k=1}^{q} \chi_k \nabla_x m_k + \chi_v \nabla_x v \right) \right] \right) \mathrm{d}y \\ & - \int_{\mathcal{P}} \left(\nabla_y \cdot \left[(\mathbf{b}(y, \mathbf{m}) - \mathbf{d}(y))\, c \right] \right) \mathrm{d}y \\ & + \int_{\mathcal{P}} \left(2^{p+1} \Phi(2y, \mathbf{u}(t, x, 2y)) c(t, x, 2y) - \Phi(y, \mathbf{u}(t, x, y)) c(t, x, y) \right) \mathrm{d}y \,.\end{aligned}$$

Since, according to (25), we have that the flux is zero in outer normal direction on the boundary of the i-state space, the second integral on the right-hand side vanishes using the divergence theorem.

Furthermore, cf. Equation (10) on page 8, using the change of variables $\tilde{y}(y) = 2y$ in the first half of the integral over the proliferation term and upon immediately dropping the tilde-sign and invoking Convention 1, we arrive for this integral at

$$\begin{aligned}&\int_{\mathcal{P}} \left(2^{p+1} \Phi(2y, \mathbf{u}(t, x, 2y)) c(t, x, 2y) - \Phi(y, \mathbf{u}(t, x, y)) c(t, x, y) \right) \mathrm{d}y \\ &\qquad = \int_{\mathcal{P}} \Phi(y, \mathbf{u}(t, x, y)) c(t, x, y) \, \mathrm{d}y \,,\end{aligned}$$

and finally, replacing the structured proliferation rate $\Phi(y, \mathbf{u})$ by its i-state-independent approximation $\bar{\Phi}(\bar{\mathbf{u}})$, we obtain

$$\approx \bar{\Phi}(\bar{\mathbf{u}}) C \,.$$

Replacing the remaining i-state-dependent parameter functions $D_c(y)$, $\chi_k(y)$ for $k = 1, \ldots, 1$, and $\chi_v(y)$ in the equation for C by their respective i-state-independent approximations $\bar{D}_c$, $\bar{\chi}_k$, and $\bar{\chi}_v$, and applying again Leibniz's

rule for differentiation under the integral sign, we obtain the following non-structured equation for the total cell density

$$\frac{\partial C}{\partial t} = \nabla_x \cdot \left[\bar{D}_c \nabla_x C - C(1-\rho(C,v)) \left(\sum_{k=1}^{q} \bar{\chi}_k \nabla_x m_k + \bar{\chi}_v \nabla_x v \right) \right] + \bar{\Phi}(\bar{\mathbf{u}}) C \,. \tag{26a}$$

We now turn to derive the non-structured counterpart of Eq. (18b), the equation for the ECM density. Making use of the non-structured approximations $\bar{\mathbf{r}}$ and $\bar{\psi}_v(t, \bar{\mathbf{u}})$ we can simply write it down as

$$\frac{\partial v}{\partial t} = -\boldsymbol{\delta}_v^{\mathsf{T}} \bar{\mathbf{r}} v + \bar{\psi}_v(t, \bar{\mathbf{u}}) \,. \tag{26b}$$

Finally, we derive the non-structured equation for the free molecular species volume concentrations and take Eq. (18c) as starting point. For the production term we use the earlier discussed approximation $\bar{\boldsymbol{\psi}}_{\mathbf{m}}(\bar{\mathbf{u}}, \bar{\mathbf{r}})$ as replacement. The term for the concentration changes due to surface binding and unbinding is approximated as follows

$$\begin{aligned} -\int_{\mathcal{P}} \left(\hat{\mathbf{b}}(y, \mathbf{m}) - \hat{\mathbf{d}}(y) \right) \varepsilon c(t,x,y) \, \mathrm{d}y &\approx -\int_{\mathcal{P}} \left(\hat{\mathbf{b}}(y, \mathbf{m}) - \hat{\mathbf{d}}(y) \right) \varepsilon \bar{c}(t,x) \, \mathrm{d}y \\ &= -\varepsilon C(t,x) \frac{1}{|\mathcal{P}|} \int_{\mathcal{P}} \left(\hat{\mathbf{b}}(y, \mathbf{m}) - \hat{\mathbf{d}}(y) \right) \mathrm{d}y \\ &= -\varepsilon C(t,x) \left(\overline{\hat{\mathbf{b}}}(\mathbf{m}) - \overline{\hat{\mathbf{d}}} \right) . \end{aligned}$$

Thus, taking that all together, we arrive at

$$\frac{\partial \mathbf{m}}{\partial t} = \nabla_x \cdot [\mathbf{D}_{\mathbf{m}} \nabla_x \mathbf{m}] - \left(\overline{\hat{\mathbf{b}}}(\mathbf{m}) - \overline{\hat{\mathbf{d}}} \right) \varepsilon C + \bar{\boldsymbol{\psi}}_{\mathbf{m}}(\bar{\mathbf{u}}, \bar{\mathbf{r}}) - \mathrm{diag}(\boldsymbol{\delta}_{\mathbf{m}}) \mathbf{m} \,. \tag{26c}$$

Finally, the initial and boundary conditions of the structured model give rise to the following initial conditions

$$C(0,x) = \int_{\mathcal{P}} c_0(x,y) \, \mathrm{d}y \,, \quad v(0,x) = v_0(x) \,, \quad \mathbf{m}(0,x) = \mathbf{m}_0(x) \quad \text{for } x \in \overline{\mathcal{D}} \,, \tag{26d}$$

and zero-flux boundary conditions

$$\begin{aligned} \left[\bar{D}_c \nabla_x C - C(1-\rho(C,v)) \left(\sum_{k=1}^{q} \bar{\chi}_k \nabla_x m_k + \bar{\chi}_v \nabla_x v \right) \right] \cdot \mathfrak{n}(x) = 0 \,, \\ [\mathbf{D}_{\mathbf{m}} \nabla_x \mathbf{m}] \cdot \mathfrak{n}(x) = \mathbf{0} \,, \\ \text{for } t \in \mathcal{I} \,,\ x \in \partial\mathcal{D} \,, \end{aligned} \tag{26e}$$

in the non-structured case.

Remark 2 We have derived above the set of non-structured equations from the structured model by deducing an equation describing the evolution of the total cell density $C(t, x)$. The total cell density is typically the observed quantity in an experimental setting and the approach taken is thus, in our view, more natural than formulating the non-structured system in terms of, e.g., the average of the structured cell density over the structure space. Furthermore, we note that different ways of arriving at non-structured models are conceivable, for instance by using appropriate quasi-steady state assumptions in the structural variable. These also make further assumptions necessary and are not followed here.

3 Application of the Modelling Framework to Cancer Invasion

In cancer modelling, most approaches exploring molecular-cell population dynamic interactions are either based on spatio-temporal PDEs of reaction-diffusion-taxis type (Gatenby and Gawlinski, 1996; Anderson et al, 2000; Byrne and Preziosi, 2004; Chaplain and Lolas, 2005; Domschke et al, 2014), or continuum-discrete hybrid systems (Anderson and Chaplain, 1998; Anderson et al, 2000; Anderson, 2005), or more recently multiscale continuum models (Ramis-Conde et al, 2008; Marciniak-Czochra and Ptashnyk, 2008; Macklin et al, 2009; Deisboeck et al, 2011; Trucu et al, 2013). Of particular interest in cancer invasion is the interaction between the tumour cell population and various proteolytic enzymes, such as MMPs (Parsons et al, 1997; Bafetti et al, 1998; Pepper, 2001; Sabeh et al, 2004, 2009) or the uPA system (Andreasen et al, 1997, 2000; Pepper, 2001), that enable the degradation of ECM components, thus promoting further local tumour progression. While the modelling of this interaction has already received special attention for the uPA system (Chaplain and Lolas, 2005, 2006; Andasari et al, 2011; Deakin and Chaplain, 2013), the structural characteristics of, in that case, the binding process of uPA to its surface receptor uPAR and the only in that state possible activation of matrix-degrading enzymes (MDEs) coupled with their simultaneous effects on cell motility and proliferation so far have been unexplored.

In this section we apply the spatio-temporal-structural modelling framework developed and described in Section 2 to derive three specific structured models that describe important aspects of the cancer cell invasion process which take cell surface binding processes of different kind and complexity into account. For these models we also derive the corresponding non-structured models according to system (26). Furthermore, we compare these derived non-structured models to models established in the literature, when available, which have been setup without having in mind the structure, i.e., accounting for these surface binding processes and their implications. Finally, we also explore the influence of the structure on the dynamics of the model components numerically for some of the models.

The models of cancer invasion to be described here follow two different schemes of action which relate the surface bound molecules to the degradation

of the ECM. In both cases, a species of diffusible (free) molecules is released by the cancer cell which may subsequently bind to the surface of cancer cells. In the first case, ECM degradation takes place *directly* by the surface-bound molecules; the free molecules are not capable of ECM degradation. According to experimental evidence, this direct scheme of action is representative for the action of MMP and MT1-MMP (which are the molecules released by the cancer cells and their membrane-tethered (MT) form, respectively) on cancer invasion and is taken up in the model described in Section 3.1. In the second case, however, ECM degradation takes place *indirectly* since these surface-bound molecules (and only these and not the free ones) firstly activate an abundantly present different molecular species from its initially inactive form to its active ECM-degradating form, which then subsequently degrades the ECM. This indirect scheme of action is representative for the uPA system, with uPA being the cancer cell released molecular species, and plasminogen and plasmin being the inactive and active form of the MDE, respectively. It is implemented in the essentially minimal model of Section 3.2 and with increased complexity in the model of the uPA system in Section 3.3.

3.1 An MT1-MMP cancer invasion model

The models given in this section are straightforward representations of the effect of MT1-MMP on cancer invasion. Evidence from the literature suggests, see (Sabeh et al, 2004, 2009), that MMPs are released by the cancer cells, diffuse in the extracellular space and can bind to the cancer cell surface. In this cell surface-bound state they are referred to as MT1-MMP. ECM degradation then takes place only by the action of this surface-bound MT1-MMP, while unbound MMP (which travels freely through the tissue) is not involved in ECM degradation. The models contain three dependent variables: the cancer cell density c, the ECM density v, and the free MMP concentration $\mathbf{m} = m_1$ (we have $q = 1$ free molecular species in these models).

In the models considered in this section, we make the following further assumptions, which are frequently used in cancer invasion modelling:

(i) free MMP undergoes natural decay at constant rate δ_{m_1};
(ii) free MMP binds to cancer cells at constant rate β;
(iii) cancer cells release free MMP at constant rate α_{m_1};
(iv) the free MMP diffusion coefficient and the cancer cell random motility coefficient are the constants D_{m_1} and D_c, respectively;
(v) cancer cells undergo haptotactic movement, obeying volume filling constraints, with respect to the ECM density at constant rate χ_v;
(vi) cancer cells proliferate logistically, obeying volume filling constraints, at constant rate μ_c;
(vii) ECM remodels locally proportional to the free space at constant rate μ_v;
(viii) ECM is degraded through the action of surface-bound MMP, that is MT1-MMP, at constant rate δ_v.

In a non-structured modelling scenario, that is without explicitly modelling the cell surface bound MT1-MMP, the three dependent variables c, v, and m_1 depend only on time and space. In that case, the binding of free MMP to the cancer cells and the subsequent degradation of the ECM can be modelled as $\delta_v c m_1 v$. This, together with the above assumptions gives rise to the following non-structured model, in non-dimensional form,

$$\frac{\partial c}{\partial t} = \nabla_x \cdot (D_c \nabla c - c(1-\rho(c,v))\chi_v \nabla v) + \mu_c c(1-\rho(c,v))\,, \tag{27a}$$

$$\frac{\partial v}{\partial t} = -\delta_v c m_1 v + \mu_v (1-\rho(c,v))^+\,, \tag{27b}$$

$$\frac{\partial m_1}{\partial t} = \nabla_x \cdot (D_{m_1} \nabla m_1) + \alpha_{m_1} c - \delta_{m_1} m_1\,. \tag{27c}$$

In the above, we define, cf. Eqs. (5) and (20), the *volume fraction of occupied space* by

$$\rho(c(t,x), v(t,x)) := c(t,x) + v(t,x)\,. \tag{27d}$$

We consider this system for $x \in \mathcal{D} = (0,X) \subset \mathbb{R}$ and for $t \in \mathcal{I} = (0,T]$ together with zero-flux boundary conditions for c and m_1 as well as the following initial conditions

$$c(0,x) = c_0(x)\,,\ v(0,x) = 1 - c_0(x)\,,\ m_1(0,x) = \frac{1}{2}c_0(x) + n_1(0,x)\,. \tag{27e}$$

Here $c_0(x)$ represents a peak of cancer cells at $x = 0$ and decays away from there whereas $n_1(0,x)$ accounts for surface-bound MT1-MMP molecules which may be present initially in a structured model. These two functions are defined together with the initial data of the structured model in Section 3.1.1 in order to have both sets of initial data consistent.

3.1.1 A structured MT1-MMP cancer invasion model

The model (27) does not capture the binding of free MMP to the cancer cell surface explicitly but rather implicitly in the ECM degradation term $-\delta_v c m_1 v$. We are now going to use our modelling framework and present a structured model where this binding is modelled explicitly. This new model will have a scalar structural variable $y = y_1 \in (0,Y)$, representing the surface concentration of the cell surface bound MT1-MMP, with Y being its maximum value. Accordingly, the cell density will now depend on time, space, and structure, i.e. $c = c(t,x,y)$. The essential new feature of this structured model is that free MMP binds to the cancer cell membrane, thus changing the structural variable y_1, and only in this bound form can unleash its potential to degrade the ECM.

We base this structured model on the general formulation given in Eqs. (18) and the assumptions listed in the beginning of Section 3.1. As before, we have the time- and space-dependent ECM density v and a single free molecular

species concentration $\mathbf{m} = m_1$, representing the free MMP concentration. Thus, in this model $p = q = 1$. Further, the generic functions contained in Eqs. (18) are specified as follows.

First, in the cell density Eq. (18a), we set the proliferation rate $\Phi(y, \mathbf{u})$ of the cancer cells such that it obeys volume filling constraints and is i-state-independent and thus takes the form

$$\Phi(y, \mathbf{u}) \equiv \Phi(C, v) = \mu_c(1 - \rho(C, v)) \,. \tag{28}$$

Furthermore, for the binding rate $\mathbf{b}(y, \mathbf{m})$, we assume that this is proportional to the available free molecular volume concentration m_1 and also proportional to the free capacity of the cell's surface, i.e. $Y - y$, and, for the unbinding rate $\mathbf{d}(y)$, we assume that this is proportional to the bound molecular surface concentration y. This gives rise to the following scalar rates with constants β and δ_y

$$\mathbf{b}(y, \mathbf{m}) = (Y - y)\beta m_1 \quad \text{and} \quad \mathbf{d}(y) = y\delta_y \,. \tag{29}$$

We only consider haptotaxis of the cells with respect to the ECM here and thus the chemotaxis coefficient $\chi_1 = 0$.

Secondly, turning our attention to the ECM density Eq. (18b), we recall that the combined vector of bound and free molecular species volume concentrations is given for this model by $\mathbf{r} = (n_1, m_1)^\mathsf{T}$ and that ECM is degraded upon contact with surface-bound MT1-MMP, that is upon contact with n_1. We assume a constant ECM degradation rate δ_v and the vector of degradation rates thus has the form

$$\boldsymbol{\delta}_v = (\delta_v, 0)^\mathsf{T} \,. \tag{30}$$

The ECM remodelling term is defined independent of the structure state y and following Eq. (15) as

$$\psi_v(t, \mathbf{u}) \equiv \psi_v(C, v) = \mu_v(1 - \rho(C, v))^+ \,. \tag{31}$$

Finally, for the free MMP concentration, that is for Eq. (18c), we consider i-state-independent linear production and degradation terms with constant coefficients, that is

$$\boldsymbol{\psi}_\mathbf{m}(\mathbf{u}, \mathbf{r}) = \boldsymbol{\psi}_\mathbf{m}(C) = \alpha_{m_1} C \qquad \text{and} \qquad \boldsymbol{\delta}_\mathbf{m} = \delta_{m_1} \,. \tag{32}$$

These considerations lead to the following structured system

$$\begin{aligned}
\frac{\partial c}{\partial t} &= \nabla_x \cdot [D_c \nabla_x c - c(1 - \rho(C, v))\chi_v \nabla_x v] - \nabla_y \cdot \big[\big((Y - y)\beta m_1 - y\delta_y\big)c\big] \\
&\quad + \mu_c(1 - \rho(C, v))\,[4c(t, x, 2y) - c(t, x, y)] \,, && \text{(33a)} \\
\frac{\partial v}{\partial t} &= -\delta_v n_1 v + \mu_v(1 - \rho(C, v))^+ \,, && \text{(33b)} \\
\frac{\partial m_1}{\partial t} &= \nabla_x \cdot [D_{m_1} \nabla_x m_1] - \Big(\big(Y\varepsilon C - n_1\big)\beta m_1 - \delta_y n_1\Big) + \alpha_{m_1} C - \delta_{m_1} m_1 \,. && \text{(33c)}
\end{aligned}$$

We consider this system for $x \in \mathcal{D} = (0, X) \subset \mathbb{R}$, $y \in \mathcal{P} = (0, Y) \subset \mathbb{R}$, $t \in \mathcal{I} = (0, T]$ and in the presence of appropriate initial and boundary conditions.

In space $\mathcal{D}$ we use zero-flux boundary conditions for c and m_1, while in the i-state space $\mathcal{P}$, due to the hyperbolic nature of the structured cell equation in the i-state variable y, we have to determine the inflow boundary $\partial\mathcal{P}_{in}(x,t)$ as defined in (23). In this example, the boundary of the i-state space is the set $\partial\mathcal{P} = \{0, Y\}$. With the corresponding outer unit normal vectors $\mathfrak{n}(0) = -1$ and $\mathfrak{n}(Y) = 1$, we obtain

$$\begin{aligned}(\mathbf{b}(0,\mathbf{m}) - \mathbf{d}(0)) \cdot \mathfrak{n}(0) &= -Y\beta m_1 \leq 0\,,\\ (\mathbf{b}(Y,\mathbf{m}) - \mathbf{d}(Y)) \cdot \mathfrak{n}(Y) &= -Y\delta_y \leq 0\,.\end{aligned}$$

Provided that there always exist free MMP molecules, i.e. $m_1 > 0$, and that binding and unbinding may take place, i.e. $\beta, \delta_y > 0$, both terms above are negative and the inflow boundary is $\partial\mathcal{P}_{in}(t,x) = \{0, Y\}$. If m_1 at some (t,x) or β or δ_y is zero, for example if we consider that no unbinding occurs, then one or both of the terms above will be zero and we do not have a classical inflow boundary at the corresponding location. Still, in such a situation, also the corresponding flux across the boundary is zero, and we make computational use of such a zero-flux boundary condition in our numerical scheme.

We set the initial structured cell density to

$$c_0(x,y) = \exp\left(-\left(x^2 + \frac{(y-y_0)^2}{y_w}\right)\frac{1}{\varepsilon^*}\right)\,. \tag{33d}$$

This represents a peak of cancer cells centred at $(x,y) = (0,y_0)$ and decaying away from there. Consequently, we obtain the initial total cell density

$$c_0(x) \equiv C(0,x) := \int_{\mathcal{P}} c_0(x,y)\,\mathrm{d}y = \gamma_1 \exp\left(-\frac{x^2}{\varepsilon^*}\right) \tag{33e}$$

and also the initial bound molecular species volume concentration

$$n_1(0,x) := \int_{\mathcal{P}} y\varepsilon c_0(x,y)\,\mathrm{d}y = \gamma_2 \exp\left(-\frac{x^2}{\varepsilon^*}\right)\,. \tag{33f}$$

The constants γ_1 and γ_2 depend here on $Y, y_0, y_w, \varepsilon, \varepsilon^*$. The functions $c_0(x)$ and $n_1(0,x)$ are precisely those which appear in the initial data of model (27). We further assume that the initial ECM density takes up the remaining free space and the initial free MMP concentration is chosen proportional to the total cell density. Thus we arrive at

$$c(0,x,y) = c_0(x,y)\,,\ v(0,x) = 1 - c_0(x)\,,\ m_1(0,x) = \frac{1}{2}c_0(x)\,. \tag{33g}$$

3.1.2 The derived non-structured MT1-MMP Cancer Invasion Model

As derived in Section 2.5 and using the mean values

$$\bar{y} = \frac{Y}{2}\,, \qquad \bar{n}_1 = \varepsilon \bar{y} C\,, \qquad \bar{\mathbf{b}}(\mathbf{m}) = (Y - \bar{y})\beta m_1\,, \quad \text{and} \qquad \bar{\mathbf{d}} = \bar{y}\delta_y\,,$$

we obtain the following non-structured model, corresponding to structured model (33),

$$\frac{\partial C}{\partial t} = \nabla_x \cdot [D_c \nabla_x C - C(1-\rho(C,v))\chi_v \nabla_x v] + \mu_c(1-\rho(C,v))C\,, \tag{34a}$$

$$\frac{\partial v}{\partial t} = -\delta_v \varepsilon \bar{y} C v + \mu_v (1-\rho(C,v))^+\,, \tag{34b}$$

$$\frac{\partial m_1}{\partial t} = \nabla_x \cdot [D_{m_1} \nabla m_1] - ((Y-\bar{y})\beta m_1 - \bar{y}\delta_y)\,\varepsilon C + \alpha_{m_1} C - \delta_{m_1} m_1\,. \tag{34c}$$

We consider this system for $x \in \mathcal{D} = (0, X) \subset \mathbb{R}$ and for $t \in \mathcal{I} = (0, T]$ together with zero-flux boundary conditions for C and m_1 as well as appropriate initial conditions, which are consistent with those used in the unstructured model (27) and those in the structured model (33). To this end, observe that in the above derived non-structured MT1-MMP model, C represents the total cell density, just like the c in the unstructured model (27). However, note that m_1 represents in the derived non-structured MT1-MMP model, as in the structured model (33), the free MMP concentration, as for binding and unbinding is accounted for through the term $((Y-\bar{y})\beta m_1 - \bar{y}\delta_y)\,\varepsilon C$. This is in contrast to the m_1 in the unstructured model (27), which represents the total (free MMP and bound MT1-MMP) concentration. Thus we consider the equations above with the following initial data, consistent with that used for models (27) and (33),

$$C(0,x) = c_0(x)\,,\ v(0,x) = 1 - c_0(x)\,,\ m_1(0,x) = \frac{1}{2}c_0(x)\,, \tag{34d}$$

where $c_0(x)$ is as in Eq. (33e).

3.1.3 Numerical Simulation Results

In this section we present in Fig. 2 numerical simulation results of the models (27), (33), and (34). In these simulations, we use the following basic parameter set ($\mathcal{S}_1$), similar to that used in Chaplain and Lolas (2005):

Domain:	$X = 6$	$Y = 1$	$T = 200$	
$c_0(x,y)$:	$y_0 = 0.25$	$y_w = 0.25$	$\varepsilon^* = 0.01$	
c :	$D_c = 3.5 \cdot 10^{-4}$	$\chi_v = 2.85 \cdot 10^{-2}$	$\mu_c = 0.15$	($\mathcal{S}_1$)
i-state :	$\varepsilon = 0.1$	$\beta = 0.2$	$\delta_y = 5 \cdot 10^{-2}$	
v :		$\delta_v = 10$	$\mu_v = 0.1$	
m_1 :	$D_{m_1} = 4.9 \cdot 10^{-3}$	$\alpha_{m_1} = 0.75$	$\delta_{m_1} = 0.1$	

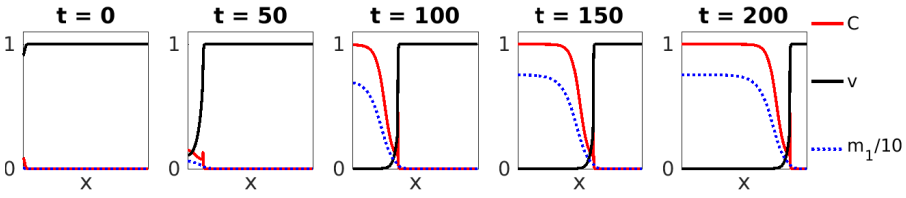

(a) initial non-structured model (27)

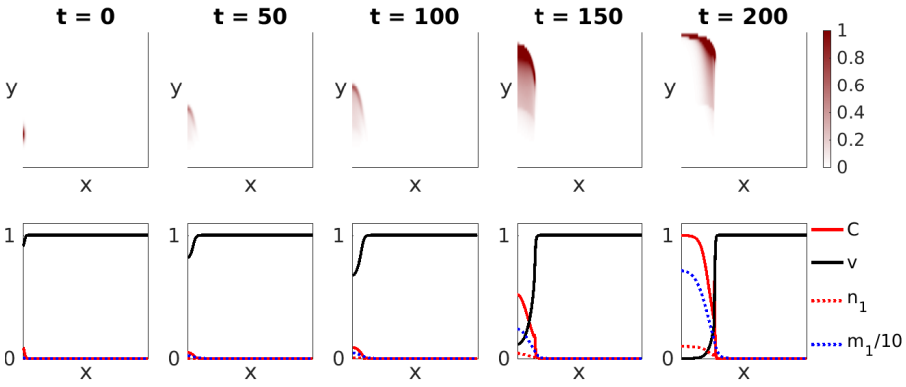

(b) structured model (33)

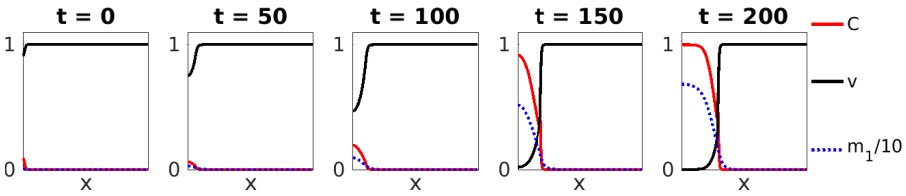

(c) derived non-structured model (34)

Figure 2: Plots showing the numerical simulation results at increasing time points (left to right) of the MT1-MMP models as specified ((a) to (c)) using the basic parameter set $\mathcal{S}_1$.

With these parameters, the cancer cells, initially concentrated at $x = 0$, do not reach the right boundary $x = X$ of $\mathcal{D}$ within the time interval $\mathcal{I}$.

The results shown in Figs. 2a and 2c are obtained from simulations of the initial non-structured model (27) and the derived non-structured model (34), respectively. In these plots we show the total cancer cell density $C(t, x)$, the ECM density $v(t, x)$, and the free molecular species volume concentrations $m_1(t, x)$ in the spatial domain $\mathcal{D}$ at initial time $t = 0$ and at times $t = 50, 100, 150$, and 200. The results shown in Fig. 2b are obtained from a simulation of the structured model (33). In these plots we show the structured cancer cell density $c(t, x, y)$ in the *spatio-structural* space $\mathcal{D} \times \mathcal{P}$ in the top row and, in the bottom row, the total cancer cell density $C(t, x)$, the ECM density $v(t, x)$, and the bound and free molecular species volume concentra-

tions $\mathbf{r}(t,x) = (n_1(t,x), m_1(t,x))^\mathsf{T}$ in the spatial domain $\mathcal{D}$ at initial time $t = 0$ and at times $t = 50, 100, 150$, and 200 (from left to right). Note that in all figures the value of m_1 is scaled by 10.

Considering first the structured model results shown in Fig. 2b (top row), we observe that, initially, only a small amount of free MMP is bound to the cell surface, thus becoming there MT1-MMP. Over time, the cancer cells proliferate, release more free MMP (m_1), and that binds to the cancer cell membrane as MT1-MMP and subsequently degrades ECM. Thus at later times, $t > 100$, the amount of MT1-MMP has increased significantly. Accordingly, ECM degradation increases also substantially past $t = 100$ as can be seen in Fig. 2b (bottom row). Qualitatively and quantitatively, that behaviour is, (up to minor differences) very well captured by the derived non-structured model (34), see Fig. 2c. The situation is much different for the initial non-structured model (27), which was setup without taking a structure into account, where we observe a much faster ECM degradation and a considerably higher cancer invasion speed. In summary, we conclude from the models and simulations in this section, that if detailed structural information is not required, then the derived non-structured model can provide (at least in this example) consistent results.

3.2 A minimal structured model of invasion with indirect ECM degradation

3.2.1 The structured model

In this section we present a structured model which implements an indirect action of a cancer cell surface-bound molecule on ECM degradation. It can be seen as an essentially minimal model of cancer invasion via the uPA system, which is described in more detail in Section 3.3, devoid of much of its complexity. In this model here, as in the first models, cf. Section 3.1, we have cancer cells releasing a molecular species and these molecules can bind to the cell surface. In contrast to the first model, these surface-bound molecules cannot degrade the ECM directly but activate an abundantly present, molecular species from its inactive to its active and ECM-degradating form, which then subsequently degrades the ECM. Therefore, for the model of this section, we have, besides a structured population of cancer cells with cell density $c(t,x,y)$ and the ECM with density $v(t,x)$, two free molecular species concentrations $m_1(t,x)$ and $m_2(t,x)$. Cancer cells proliferate and rearrange spatially through random motility and haptotaxis with respect to v. The first molecular species, m_1, is produced by the cancer cells and can bind to the surface of the cells; the latter process gives rise to the i-state of a cell. The second molecular species, m_2, is solely produced (or activated from an abundantly present inactive form) through the action of bound molecules of the first type and degrades the ECM. Thus in this model we have $p = 1$ and $q = 2$. Accordingly, the one-dimensional i-state space $\mathcal{P} = (0, Y)$, where $Y > 0$ denotes the

maximum surface concentration of m_1. We detail our assumptions regarding the coefficients and parameters of the general model (18) in the following.

For the structured cell density equation (18a), we use the cell random motility constant D_c and vanishing chemotaxis coefficients $\chi_1 = \chi_2 = 0$. The haptotaxis coefficient $\chi_v(y)$ is chosen i-state-dependent in order to account for the effect that free receptors for m_1 on the cell surface may bind to the ECM and thus accelerate haptotactic cell migration; for details we refer to the numerical simulations in this section. The proliferation rate $\Phi(y, \mathbf{u})$ of the cancer cells as well as the scalar binding rate $\mathbf{b}(y, \mathbf{m})$ and the scalar unbinding rate $\mathbf{d}(y)$ are chosen with the same considerations as in the structured model in Section 3.1, and thus take the form as given in Eqs. (28) and (29), respectively.

Turning to the ECM density equation (18b), the combined vector of bound and free molecular species volume concentrations is given, for this model, by $\mathbf{r} = (n_1, m_1, m_2)^T \in \mathbb{R}^3$ and ECM is degraded upon contact with m_2. We assume a constant ECM degradation rate δ_v and the vector of degradation rates has thus the form

$$\boldsymbol{\delta}_v^{\mathsf{T}} = (0, 0, \delta_v)\,. \tag{35}$$

The remodelling term is defined independent of y and as given in Eq. (31).

Finally, in Eq. (18c) for $\mathbf{m}$, we consider the following linear production and degradation terms with constant coefficients

$$\boldsymbol{\psi}_{\mathbf{m}}(\mathbf{u}, \mathbf{r}) = \begin{pmatrix} \alpha_{m_1} C \\ \alpha_{m_2} n_1 \end{pmatrix} \qquad \text{and} \qquad \boldsymbol{\delta}_{\mathbf{m}} = \begin{pmatrix} \delta_{m_1} \\ \delta_{m_2} \end{pmatrix}. \tag{36}$$

In the above production term $\alpha_{m_2} n_1$ of m_2 we have now explicitly modelled that only surface-bound molecules, represented by n_1 can activate the inactive MDE to its active form m_2. In that way, the production term of m_2 depends implicitly on the i-state.

These considerations lead to the following structured system

$$\begin{aligned}
\frac{\partial c}{\partial t} &= \nabla_x \cdot [D_c \nabla_x c - c(1-\rho(C,v))\chi_v(y)\nabla_x v] - \nabla_y \cdot \big[\big((Y-y)\beta m_1 - y\delta_y\big)c\big] \\
&\quad + \mu_c(1-\rho(C,v))\,[4c(t,x,2y) - c(t,x,y)]\,, && \text{(37a)} \\
\frac{\partial v}{\partial t} &= -\delta_v m_2 v + \mu_v(1-\rho(C,v))^+\,, && \text{(37b)} \\
\frac{\partial m_1}{\partial t} &= \nabla_x \cdot [D_{m_1} \nabla_x m_1] - \Big(\big(Y\varepsilon C - n_1\big)\beta m_1 - \delta_y n_1\Big) + \alpha_{m_1} C - \delta_{m_1} m_1\,, && \text{(37c)} \\
\frac{\partial m_2}{\partial t} &= \nabla_x \cdot [D_{m_2} \nabla_x m_2] + \alpha_{m_2} n_1 - \delta_{m_2} m_2\,. && \text{(37d)}
\end{aligned}$$

We consider this system for $x \in \mathcal{D} = (0, X) \subset \mathbb{R}$, $y \in \mathcal{P} = (0, Y) \subset \mathbb{R}$, and for $t \in \mathcal{I} = (0, T]$ together with appropriate initial and boundary conditions.

In space $\mathcal{D}$ we have zero-flux boundary conditions for c, m_1, and m_2. Observe that the inflow boundary in the i-state space $\mathcal{P}$ is the same as in the MT1-MMP cancer invasion model, see Section 3.1.1, that is $\partial\mathcal{P}_{in}(t, x) = \{0, Y\}$,

provided that there always exist molecules of the first type, i.e. $m_1 > 0$, and that binding and unbinding may take place, i.e. $\beta, \delta_y > 0$. If one of these conditions is not satisfied at a boundary point then, as in Section 3.1.1, the boundary point is not an inflow boundary but still the flux across it is zero. Again, we make computational use of such a zero-flux boundary condition in our numerical scheme.

We use the same initial structured and total cell density, $c_0(x, y)$ and $c_0(x)$, respectively as given in Eqs. (33d, 33e) and the following initial conditions

$$c(0, x, y) = c_0(x, y)\,,\ v(0, x) = 1 - c_0(x)\,,\ \mathbf{m}(0, x) = \left(\frac{1}{2}c_0(x), 0\right)^{\mathsf{T}}\,. \quad (37e)$$

3.2.2 The derived non-structured model

Following Section 2.5, we now derive a corresponding non-structured model to system (37). Using the mean value $\bar{\chi}_v$ of the i-state-dependent coefficient $\chi_v(y)$ and the mean values

$$\bar{y} = \frac{Y}{2}\,, \qquad \bar{n}_1 = \varepsilon \bar{y} C\,, \qquad \bar{\mathbf{b}}(\mathbf{m}) = (Y - \bar{y})\beta m_1\,, \quad \text{and} \qquad \bar{\mathbf{d}} = \bar{y}\delta_y\,,$$

we obtain

$$\frac{\partial C}{\partial t} = \nabla_x \cdot [D_c \nabla_x C - C(1 - \rho(C, v))\bar{\chi}_v \nabla_x v] + \mu_c(1 - \rho(C, v))C\,, \quad (38a)$$

$$\frac{\partial v}{\partial t} = -\delta_v m_2 v + \mu_v(1 - \rho(C, v))^+\,, \quad (38b)$$

$$\frac{\partial m_1}{\partial t} = \nabla_x \cdot [D_{m_1} \nabla m_1] - ((Y - \bar{y})\beta m_1 - \bar{y}\delta_y)\,\varepsilon C + \alpha_{m_1} C - \delta_{m_1} m_1\,, \quad (38c)$$

$$\frac{\partial m_2}{\partial t} = \nabla_x \cdot [D_{m_2} \nabla m_2] + \alpha_{m_2} \varepsilon \bar{y} C - \delta_{m_2} m_2\,. \quad (38d)$$

We consider this system for $x \in \mathcal{D} = (0, X) \subset \mathbb{R}$ and for $t \in \mathcal{I} = (0, T]$ together with zero-flux boundary conditions for C, m_1 and m_2 as well as appropriate initial conditions, which are consistent with those used in the structured model (37), that is

$$C(0, x) = c_0(x)\,,\ v(0, x) = 1 - c_0(x)\,,\ \mathbf{m}(0, x) = \left(\frac{1}{2}c_0(x), 0\right)^{\mathsf{T}}\,. \quad (38e)$$

3.2.3 Numerical simulations results

The simulations in this section highlight the difference that the structural binding information makes in characterising the dynamics in the structured

case (37) versus the corresponding non-structured system (38). In these numerical simulations, we use the following basic parameter set $\mathcal{S}_2$ similar to that used in Chaplain and Lolas (2005):

$$
\begin{array}{rccc}
\text{Domain:} & X = 6 & Y = 1 & T = 200 \\
c_0(x,y): & y_0 = 0.25 & y_w = 0.25 & \varepsilon^* = 0.01 \\
c: & D_c = 3.5 \cdot 10^{-4} & \bar{\chi}_v = 2.85 \cdot 10^{-2} & \mu_c = 0.15 \\
i\text{-state}: & \varepsilon = 0.1 & \beta = 0.2 & \delta_y = 0 \\
v: & & \delta_v = 10 & \mu_v = 0.1 \\
m_1: & D_{m_1} = 2.5 \cdot 10^{-3} & \alpha_{m_1} = 0.215 & \delta_{m_1} = 0.1 \\
m_2: & D_{m_2} = 4.91 \cdot 10^{-3} & \alpha_{m_2} = 0.75 & \delta_{m_2} = 0.1
\end{array}
\qquad (\mathcal{S}_2)
$$

For the structured case, we consider also the haptotaxis coefficient χ_v as a function linearly decaying from a maximal value χ_v^+ for $y = 0$ to a minimal value χ_v^- for $y = Y$ in order to model the effect that free receptors may bind to the ECM and thus accelerate haptotactic movement. Apposite to the basic parameter set $\mathcal{S}_2$, we thus choose

$$
\chi_v(y) = (\chi_v^- - \chi_v^+)\frac{y}{Y} + \chi_v^+ , \quad \chi_v^- = 0.001 , \quad \chi_v^+ = 0.056 . \qquad (39)
$$

This leads to the mean haptotactic coefficient equal to 0.0285, which is identical with $\bar{\chi}_v$ from the basic parameter set $\mathcal{S}_2$.

The results shown in Figures 3 and 5, are obtained from simulations of the structured model (37) using the parameter set $\mathcal{S}_2$ with modifications as detailed in each figure caption. They present the structured cancer cell density $c(t,x,y)$ in the *spatio-structural* space $\mathcal{D} \times \mathcal{P}$ in the top row and, in the bottom row, the total cancer cell density $C(t,x)$, the ECM density $v(t,x)$, and the bound and free molecular species volume concentrations $\mathbf{r}(t,x)$ in the spatial domain $\mathcal{D}$ at initial time $t = 0$ and at times $t = 50, 100, 150$, and 200 (from left to right).

The results shown in Figure 4 are obtained from a simulation of the corresponding derived non-structured model (38) using parameters according to $\mathcal{S}_2$. They present the total cancer cell density $C(t,x)$, the ECM density $v(t,x)$, and the free molecular species volume concentrations $\mathbf{m}(t,x)$ in the spatial domain $\mathcal{D}$ at initial time $t = 0$ and at times $t = 50, 100, 150$, and 200 (from left to right).

In Figure 3a, we see that initially only a small amount of molecules of m_1 is bound to the cancer cell surface and hence the ECM is degraded much more slowly than in the corresponding non-structured case in Figure 4. Over time, the cancer cells proliferate, produce, and bind more of the m_1-molecules, which in turn activate the MDE m_2. Hence, at later times, the level of MDEs m_2 is about twice as much in the structured case as in the non-structured case shown in Figure 4.

A comparison between the spatio-structural dynamics shown in the top rows of Figures 3a and 3b reveals that until $t = 150$ the amount of bound m_1-molecules, i.e. n_1, is less in the i-state-dependent case, leading to a slower

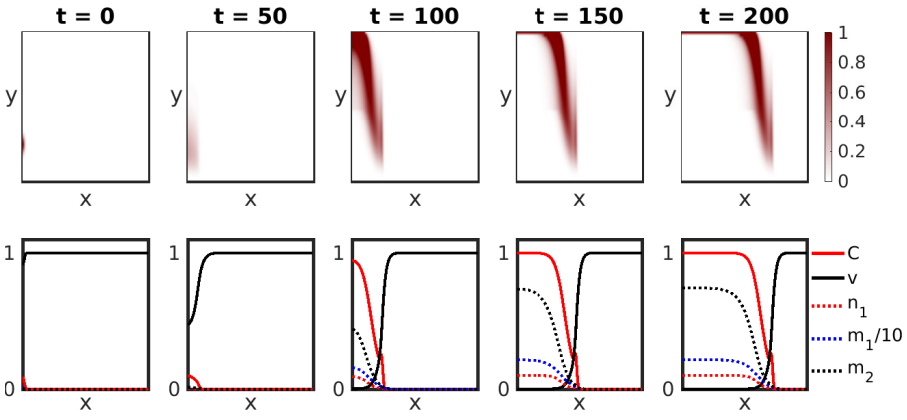

(a) constant χ_v

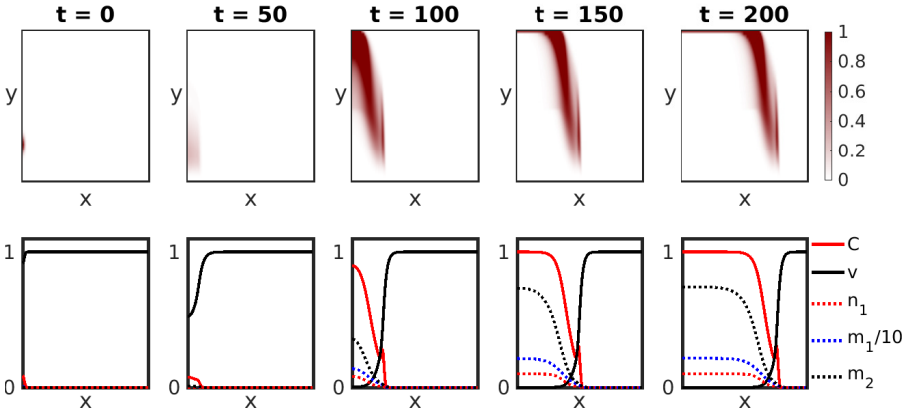

(b) i-state-dependent χ_v, cf. (39)

Figure 3: Plots showing the computational simulation results at increasing time points (left to right) of the structured system (37) using the basic parameter set $\mathcal{S}_2$ with the haptotaxis term χ_v as specified in (a) and (b). The top row in each of (a) and (b) shows the evolution of the structured cancer cell density in the spatio-structural space $\mathcal{D} \times \mathcal{P}$; the bottom row in each of (a) and (b) shows the evolution of all non-structured variables in the spatial domain $\mathcal{D}$.

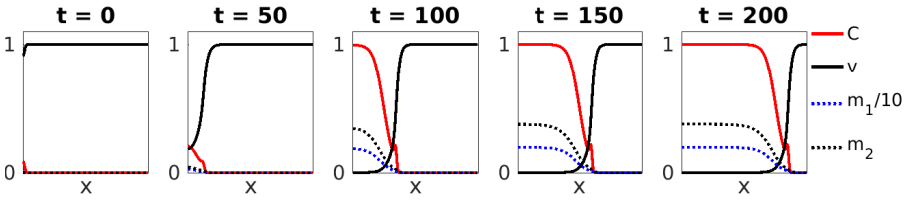

Figure 4: Plots showing the computational simulation results at increasing time points (left to right) of the derived non-structured system (38) using the basic parameter set $\mathcal{S}_2$.

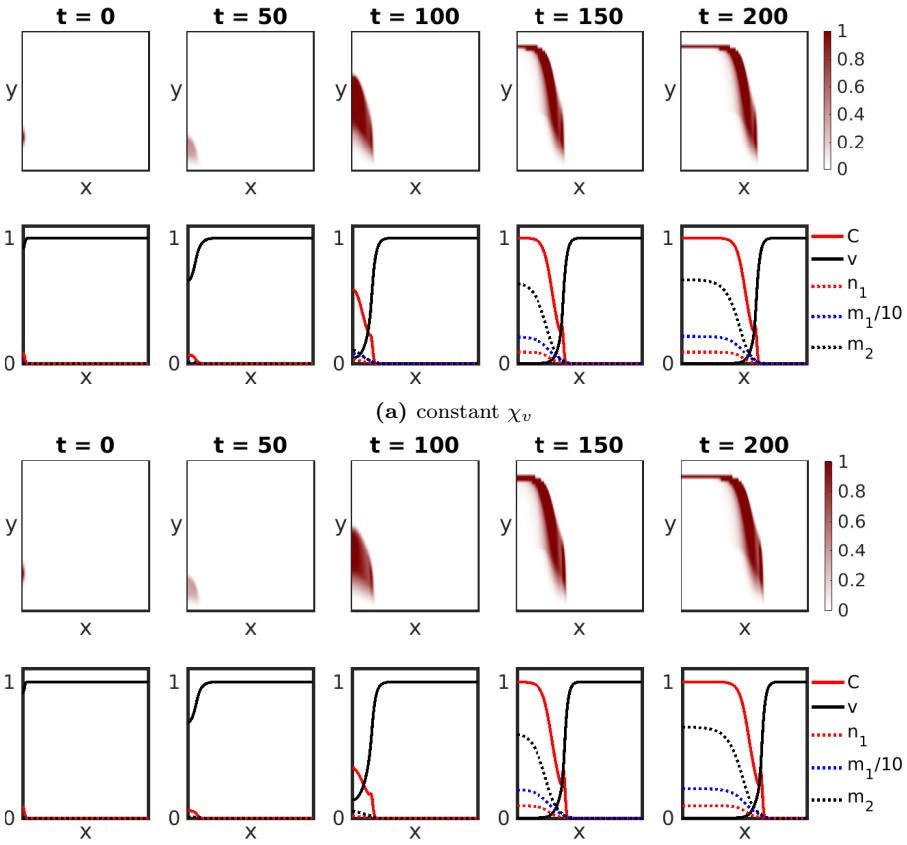

(a) constant χ_v

(b) i-state-dependent χ_v

Figure 5: Plots showing the computational simulation results at increasing time points (left to right) of the structured system (37) using the basic parameter set $\mathcal{S}_2$ with unbinding of molecules at the rate $\delta_y = 0.05$ and using the haptotaxis term χ_v as specified in (a) and (b). The top row in each of (a) and (b) shows the evolution of the structured cancer cell density in the spatio-structural space $\mathcal{D} \times \mathcal{P}$; the bottom row in each of (a) and (b) shows the evolution of all non-structured variables in the spatial domain $\mathcal{D}$.

start in ECM degradation while the cancer cells $c(t, x, y)$ remain less spread in the structural variable.

In Figure 5 we present the simulation results of the model (37), where we consider the unbinding of molecules from the cell surface with rate $\delta_y = 0.05$. We observe that due to the unbinding of the m_1-molecules, the degradation of the ECM is less compared to the case without unbinding, and the cell-surface concentration remains below the maximum of 1, i.e., $y < 1$. A stronger aggregating tendency in the i-state component of the spatio-structural distribution of the invading cancer cells can be observed in Figure 5, with the leading peak being higher compared to that in Figure 3.

3.3 A Structured-Population Model of Cancer Invasion Based on the uPA System

After exploring, in the previous section, the structured-population framework for a simplified model of cancer invasion inspired by the uPA system, we now apply this framework to setup a more involved model of cancer invasion using the full uPA scheme. We will also present the corresponding non-structured model and compare it to an already existing model for the same process.

Cancer cell invasion is a complex process occurring across many scales, both spatial and temporal, ranging from biochemical intracellular interactions to cellular and tissue scale processes. A major component of the invasive process is the degradation of the extracellular matrix (ECM) by proteolytic enzymes. One important enzymatic system in cancer invasion that has been investigated in the literature is the so-called uPA system (urokinase plasminogen activation system), see for example Chaplain and Lolas (2005, 2006); Andasari et al (2011). It consists of a cancer cell population, the ECM, urokinase plasminogen activator (uPA) alongside plasminogen activator inhibitor type-1 (PAI-1) proteins, and the matrix degrading enzyme plasmin. These are accompanied by urokinase plasminogen activator receptor (uPAR) molecules that are located on the cancer cell membrane.

The free uPA molecules bind to uPAR and this complex subsequently activates the matrix degrading enzyme plasmin from its pro-enzyme plasminogen. In healthy cells, the activation of plasminogen is tightly regulated by the availability of uPA, for example by producing inhibitors of uPA like PAI-1. In contrast, cancer cells produce uPA to activate plasminogen, and hence excessively degrade the ECM, this way making room for further invasion. A schematic diagram can be found in Figure 6a. Details about the uPA system from a biological point of view can be found for example in Andreasen et al (1997); Duffy (2004); Ulisse et al (2009).

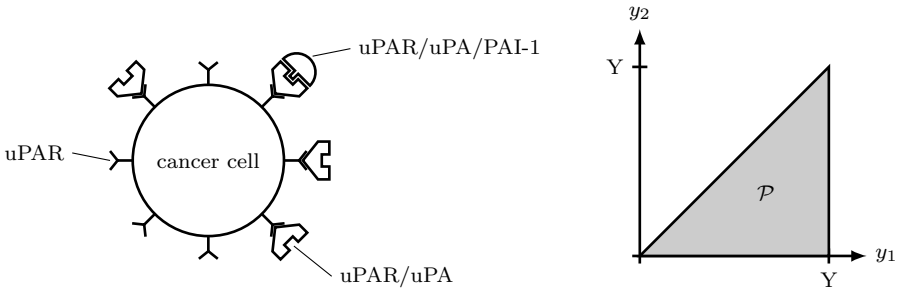

(a) **(b)**

Figure 6: Schematic diagrams of (a) a cancer cell with surface-bound receptors uPAR, bound uPA and inhibitor PAI-1; (b) the corresponding i-state space $\mathcal{P}$.

Our structured general modelling framework (18) specialises for the uPA system using the following dependent variables:

- the structured cancer cell density $c(t, x, y)$;
- the extracellular matrix density $v(t, x)$;
- the free molecular species volume concentrations $\mathbf{m} = (m_1, m_2, m_3)^\mathsf{T}$, where $m_1(t, x)$ represents the uPA, $m_2(t, x)$ stands for the PAI-1, and $m_3(t, x)$ is the plasmin volume concentration.

Here we assume that cancer cells carry a fixed amount of uPAR bound to their surface, hence the binding of uPA to the surface is limited by a maximal surface concentration Y. Free PAI-1 enzymes only bind to the bound uPA. The two-dimensional i-state $y = (y_1, y_2)^\mathsf{T} \in \mathcal{P}$ therefore consists of the surface concentration y_1 of bound uPA on the cell surface, and the surface concentration $y_2 \leq y_1$ of bound inhibitor PAI-1 molecules attached to the bound uPA enzymes. Hence, the i-state space $\mathcal{P}$ is given by the open triangle $\mathcal{P} = \{y \in (0, Y)^2 : y_2 < y_1\}$, as illustrated in the schematic diagram shown in Figure 6b.

For the binding rate of uPA, b_1, we assume that it is proportional to the free (unoccupied) receptors $Y - y_1$ and also to the availability of the free uPA, m_1. The binding rate of the inhibitor PAI-1, b_2, is assumed to be proportional to the uninhibited bound uPA $y_1 - y_2$ and the availability of free PAI-1. Similarly, we assume the unbinding rate d_2 of PAI-1 to be proportional to the bound PAI-1, i.e., y_2. In this model, we do not consider that a uPA/PAI-1 complex unbinds as a whole but that first the PAI-1 must unbind. Hence, the unbinding rate d_1 of uPA is proportional to the bound but uninhibited uPA, i.e. $y_1 - y_2$. This gives rise to the following rates

$$\mathbf{b}(y, \mathbf{m}) = \begin{pmatrix} (Y - y_1)\beta_1 m_1 \\ (y_1 - y_2)\beta_2 m_2 \end{pmatrix}, \qquad \text{and} \qquad \mathbf{d}(y) = \begin{pmatrix} (y_1 - y_2)\delta_{y_1} \\ y_2 \delta_{y_2} \end{pmatrix}. \tag{40}$$

While the uPA is produced by the cancer cells, and the inhibitor PAI-1 is produced via plasmin activation, plasmin itself is activated from plasminogen by uninhibited bound uPA, which is described by $n_1 - n_2$. Hence, with $\mathbf{u}$ and $\mathbf{r}$ defined in (4), we obtain that the vector of linear production terms is given by

$$\boldsymbol{\psi}_{\mathbf{m}}(\mathbf{u}, \mathbf{r}) = \begin{pmatrix} \alpha_{m_1} C \\ \alpha_{m_2} m_3 \\ \alpha_{m_3}(n_1 - n_2) \end{pmatrix}.$$

Finally, using the i-state-independent logistic proliferation law $\Phi(C,v)$ defined in (28), we arrive at the following system

$$\begin{aligned}\frac{\partial c}{\partial t} &= \nabla_x\cdot\Big(D_c\nabla_x c - c(1-\rho(C,v))\left(\chi_1\nabla_x m_1 + \chi_2\nabla_x m_2 + \chi_v\nabla_x v\right)\Big)\\ &\quad - \nabla_y\cdot\Big((\mathbf{b}(y,\mathbf{m})-\mathbf{d}(y))c\Big) + \Phi(C,v)\left(8c(t,x,2y) - c(t,x,y)\right)\,,\end{aligned} \tag{41a}$$

$$\frac{\partial v}{\partial t} = -\delta_v m_3 v + \mu_v(1-\rho(C,v))^+\,, \tag{41b}$$

$$\begin{aligned}\frac{\partial m_1}{\partial t} &= \nabla_x\cdot[D_{m_1}\nabla_x m_1] - \big((Y\varepsilon C - n_1)\beta_1 m_1 - (n_1-n_2)\delta_{y_1}\big)\\ &\quad + \alpha_{m_1}C - \delta_{m_1}m_1\,,\end{aligned} \tag{41c}$$

$$\frac{\partial m_2}{\partial t} = \nabla_x\cdot[D_{m_2}\nabla_x m_2] - \big((n_1-n_2)\beta_2 m_2 - n_2\delta_{y_2}\big) + \alpha_{m_2}m_3 - \delta_{m_2}m_2\,, \tag{41d}$$

$$\frac{\partial m_3}{\partial t} = \nabla_x\cdot[D_{m_3}\nabla_x m_3] + \alpha_{m_3}(n_1-n_2) - \delta_{m_3}m_3\,. \tag{41e}$$

As before, system (41) is supposed to hold for $t\in\mathcal{I}$, $x\in\mathcal{D}$ and $y\in\mathcal{P}$ and is completed by initial conditions and appropriate boundary conditions. In space we have again zero-flux boundary conditions, while we have to determine the inflow boundary $\partial\mathcal{P}_{in}(t,x)$ as defined in (23) for the i-state space. Here, the i-state space is defined as a triangle, see Fig. 6b, and we can divide the boundary into three parts, $\partial\mathcal{P} = \overline{\partial\mathcal{P}_1\cup\partial\mathcal{P}_2\cup\partial\mathcal{P}_3}$ with $\partial\mathcal{P}_1 := \{(y_1,0) : 0 < y_1 < Y\}$, $\partial\mathcal{P}_2 := \{(Y,y_2) : 0 < y_2 < Y\}$, and $\partial\mathcal{P}_3 := \{(y_1,y_1) : 0 < y_1 < Y\}$, and the corresponding outer unit normal vectors

$$\mathfrak{n}(y) = \begin{cases}(0,-1)^\mathsf{T}\,, & \text{for } y\in\partial\mathcal{P}_1\,,\\ (1,0)^\mathsf{T}\,, & \text{for } y\in\partial\mathcal{P}_2\,,\\ \frac{1}{\sqrt{2}}(-1,1)^\mathsf{T}\,, & \text{for } y\in\partial\mathcal{P}_3\,.\end{cases}$$

Then we obtain

$$(\mathbf{b}(y,\mathbf{m}-\mathbf{d}(y))\cdot\mathfrak{n}(y) = \begin{cases}-y_1\beta_2 m_2 \le 0\,, & \text{for } y\in\partial\mathcal{P}_1\,,\\ -(Y-y_2)\delta_{y_1}\le 0\,, & \text{for } y\in\partial\mathcal{P}_2\,,\\ -\frac{1}{\sqrt{2}}\left((Y-y_1)\beta_1 m_1 + y_1\delta_{y_2}\right)\le 0\,, & \text{for } y\in\partial\mathcal{P}_3\,.\end{cases}$$

Provided that there exist molecules of the first and second type (meaning that the volume concentrations $m_1(t,x)$ and $m_2(t,x)$ are positive) and that binding and unbinding may take place (meaning that the binding and unbinding rate parameters $\beta_{1/2}$ and $\delta_{y_{1/2}}$ are positive), all terms above are negative and the inflow boundary is $\partial\mathcal{P}_{in}(t,x) = \partial\mathcal{P}$. In case $m_1(t,x)$ or $m_2(t,x)$ or some of the parameters are zero, we might not have a classical inflow boundary at some parts of $\partial\mathcal{P}$.

As derived in Section 2.5 and using the mean values of the i-state-dependent coefficients,

$$\bar{y} = \begin{pmatrix} \frac{2}{3}Y \\ \frac{1}{3}Y \end{pmatrix}, \quad \bar{\mathbf{b}}(\mathbf{m}) = \begin{pmatrix} (Y-\bar{y}_1)\beta_1 m_1 \\ (\bar{y}_1-\bar{y}_2)\beta_2 m_2 \end{pmatrix}, \quad \bar{\mathbf{d}} = \begin{pmatrix} (\bar{y}_1-\bar{y}_2)\delta_{y_1} \\ \bar{y}_2\delta_{y_2} \end{pmatrix},$$

we obtain the following corresponding non-structured model for the dynamics of the uPA system

$$\begin{aligned} \frac{\partial C}{\partial t} &= \nabla_x\cdot\Big(\bar{D}_c\nabla_x C - C(1-\rho(C,v))(\bar{\chi}_1\nabla_x m_1 + \bar{\chi}_2\nabla_x m_2 + \bar{\chi}_v\nabla_x v)\Big) \\ &\quad + \Phi(C,v)C\,, \end{aligned} \tag{42a}$$

$$\frac{\partial v}{\partial t} = -\delta_v m_3 v + \mu_v(1-\rho(C,v))^+\,, \tag{42b}$$

$$\begin{aligned} \frac{\partial m_1}{\partial t} &= \nabla_x\cdot[D_{m_1}\nabla_x m_1] - \big((Y-\bar{y}_1)\beta_1 m_1 - (\bar{y}_1-\bar{y}_2)\delta_{y_1}\big)\varepsilon C \\ &\quad + \alpha_{m_1}C - \delta_{m_1}m_1\,, \end{aligned} \tag{42c}$$

$$\frac{\partial m_2}{\partial t} = \nabla_x\cdot[D_{m_2}\nabla_x m_2] - ((\bar{y}_1-\bar{y}_2)\beta_2 m_2 - \bar{y}_2\delta_{y_2})\varepsilon C + \alpha_{m_2}m_3 - \delta_{m_2}m_2\,, \tag{42d}$$

$$\frac{\partial m_3}{\partial t} = \nabla_x\cdot[D_{m_3}\nabla_x m_3] + (\bar{y}_1-\bar{y}_2)\alpha_{m_3}\varepsilon C - \delta_{m_3}m_3\,. \tag{42e}$$

The unstructured system (42) obtained this way is similar in flavour to the one initially proposed by Chaplain and Lolas (2005, 2006). The first differences appear though in equation (42b) and are due to the fact that our general structured framework (18) assumed the simplified scenario for the ECM concentration evolution that is based only on enzymatic degradation and volume filling remodelling. In their special model (Chaplain and Lolas, 2005, 2006), the binding and unbinding of the PAI-1 inhibitor to and from the ECM as well as to and from the free uPA is taken into account, as well. These aspects show up also in the subsequent equations of the model proposed in Chaplain and Lolas (2005, 2006) concerning the dynamics of uPA, PAI-1, and plasmin, which cause them to differ in this regard from (42c)-(42e).

On the other hand, while in (42d) the process of PAI-1 inhibitor m_2 leaving the system through binding to the surface-bound uPA is captured by the structured framework (41d), in the corresponding equation from Chaplain and Lolas (2005, 2006) this is modelled by having the PAI-1 binding to the free uPA. Also, while Chaplain and Lolas (2005, 2006) assume a co-localisation of uPA and uPAR to activate plasmin, in our structured case (41e), the plasmin m_3 is explicitly activated by uninhibited bound uPA $n_1 - n_2$, this leading to the non-structured approximation (42e) expressed by a quantitatively derived proportionality to the cell surface distribution εC. Future work will explore further similarities and discrepancies between the proposed structured and

non-structured uPA models in an integrated computational and analytic approach.

4 Conclusions and Outlook

In this paper we have established a general *spatio-temporal-structural* framework that allows to describe the interaction of cell population dynamics (i.e. cell movement and proliferation) with molecular binding processes. Any such structured model is complemented with a corresponding non-structured, spatio-temporal model. The latter is obtained by integrating the structured model over its i-state space. Three specific examples, motivated by the process of cancer invasion, illustrate the applicability of the general structured framework and highlight the differences to the corresponding non-structured models.

In the first example, we modelled cancer invasion on the basis of experimental evidence that only surface-bound MMP, referred to as MT1-MMP, can degrade the ECM. Here surface-bound molecules directly acted as matrix degrading enzymes. Our investigation has highlighted that generally adopting only a spatio-temporal approach in setting up a non-structured model may not capture the process as faithfully as described by an appropriately derived structured model. However, our derived non-structured model, which implicitly captures part of the binding/unbinding process, provides simulation results which are in very good agreement with results from the structured model. Thus, in this case, the structured modelling framework proposed in this work has led the way to an appropriate non-structured model.

In the second example, a minimal model of cancer invasion is presented where the surface-bound molecules do not directly degrade the ECM but indirectly via the activation of an MDE from its inactive from. This indirect type of action is reminiscent of the uPA system, which is treated as third example. We observe numerically that the overall dynamics of the structured model differs in some regard from the corresponding non-structured one. This finds expression, for example, in a slower or faster degradation of the ECM depending on the amount of bound molecules, a different shape, speed, and intensity of the invading front, or different levels of the free matrix-degrading molecules.

In the third example, a model for the uPA-system, we compare the corresponding non-structured model with an existing non-structured model from Chaplain and Lolas (2005, 2006). Our structured model is a more faithful representation of the underlying biology and structural information is inherited by the corresponding non-structured model and may lead to different terms compared to the existing non-structured model. This is evident, for example, in the term modelling the activation of plasmin, which is, as described in the biological literature, activated by cell-membrane bound but uninhibited uPA. While the model from the literature assumes activation via co-localisation of uPA and cancer cells (i.e. uPAR) but does not directly account for the binding to the cell membrane, our non-structured model uses the i-state mean

value of the uninhibited bound uPA, thus this actually incorporates structural information in a condensed form. Also, while in the existing non-structured model free uPA and PAI-1 are removed from the system upon contact as free uPA/PAI-1 complexes, they bind to the cell membrane and accordingly reduce the free uPA and PAI-1 volume concentration in our case; the internalisation of the uPAR/uPA/PAI-1 complex by the cell is discussed further below.

The benefit of this general structured model is that complex biological processes like binding to or unbinding from the cell's surface can be modelled quite naturally. We are able to distinguish between free and bound molecules, which can induce different reaction processes as was motivated biologically by the uPA system. Further, the bound molecules implicitly move with the cells, while the free molecules follow their own Brownian motion. Moreover, the corresponding non-structured model, being an approximation of the structured one, inherits some of the structural information. Although the structured ansatz is computationally more expensive due to the additional dimensions of the i-state space, it allows a more realistic modelling of the underlying biological processes.

The derivation of the general structured model (18) as well as the corresponding non-structured model (26) is based on a number of assumptions and simplifications. We comment on a selection of these in some detail below but leave their thorough discussion for follow-up work.

Spatial flux generalisations. In the general model (18), we use, for the structured cell density c, the spatial flux term (12), which consists of a combination of diffusion, chemotaxis, and haptotaxis.

The diffusive flux term in (12) is chosen as $-D_c\nabla_x c$. The same form is used, for instance, in the work of Laurençot and Walker (2008), who consider an age-structured spatio-temporal model for *proteus mirabilis* swarm-colony development. This form implies that the random motility of cells with a particular i-state y depends only on the gradient of the density of cells having that same i-state. Instead, one could also think of random motility of cells at a particular i-state y which is governed by the gradient of the total cell density. This would lead to a diffusive flux term of the form $-D_c\nabla_x C$.

A further generalisation of the spatial flux term is to consider cell movement due to cell-cell and cell-matrix adhesive interactions, as is done in a non-structured situation in Armstrong et al (2006) and Gerisch and Chaplain (2008). The formulation of the required, so-called adhesion velocity $\mathcal{A}$ will then have to be extended to the structured case and could be defined as

$$\mathcal{A}(t,x,y,\mathbf{u}(t,\cdot)) = \frac{1}{R}\int\limits_{B(0,R)} \mathfrak{n}(\tilde{x})\Omega(\|\tilde{x}\|_2)g(t,y,\mathbf{u}(t,x+\tilde{x}))\,\mathrm{d}\tilde{x}$$

with the sensing radius $R>0$, $\mathfrak{n}(\tilde{x})$ a unit normal vector pointing from x to $x+\tilde{x}$, and the radial dependency function $\Omega(r)$. Similar as in the discussion for the diffusive flux above, cell adhesion occurs not only between cells of the same i-state but between cells of all i-states. Assuming the adhesive strength

to be identical for cells of all i-states, the adhesion coefficient function g will have the form

$$g(t, \mathbf{u}) \equiv \mathbf{g}(t, C, v) = [S_{cc}(t)C + S_{cv}(t)v] \cdot (1 - \rho(C, v))^+ \ ,$$

where we have that $S_{cc}(t)$ represents the cell-cell adhesion coefficient, and $S_{cv}(t)$ denotes the cell-matrix adhesion coefficient. This i-state-independent adhesion coefficient function coincides with the original one from Armstrong et al (2006) and Gerisch and Chaplain (2008), and the time-dependent extension as studied in Domschke et al (2014). In the structured case, cell-cell and cell-matrix adhesion can be influenced by the i-state of the cells, hence the adhesion coefficients would also depend on the i-state(s). In order to take all i-states into account, we have to integrate the cell-cell adhesion term over the i-state space. The adhesion coefficient function will then have the form

$$g(t, y, \mathbf{u}(t, x^*)) = \left(\int_{\mathcal{P}} S_{cc}(t, y, \tilde{y}) c(t, x^*, \tilde{y}) \, \mathrm{d}\tilde{y} + S_{cv}(t, y) v(t, x^*) \right) \cdot \Big(1 - \rho\big(C(t, x^*), v(t, x^*)\big) \Big)^+ ,$$

where $S_{cc}(t, y, \tilde{y})$ represents the cell-cell adhesion coefficient between cells of i-states y and $\tilde{y}$, respectively. $S_{cv}(t, y)$ denotes the cell-matrix adhesion coefficient of cells with i-state y and the ECM. Both extensions of the spatial flux term need to be analysed in more detail and are subject to further investigation.

Internalisation. In the general model (18) we describe how binding and unbinding of the molecules influence the dynamics of the overall system. Free molecules leave and enter the system due to binding and unbinding, while the structured cell population "moves" through the i-state space. In Cubellis et al (1990), it is described that surface-bound uPA/uPAR complexes are internalised and degraded by the cells. To include this mechanism in our model, we would have to add an internalisation term, similar to the unbinding term, to the structural flux (14). Since the uPA/uPAR complexes are degraded, they would not reenter the system as they do in the case of unbinding, hence the internalisation term would not appear in the free molecular species equation (18c).

Variable receptor density. In the special case of the uPA system, we assume, following the work of Chaplain and Lolas (2005, 2006), that a cancer cell carries a fixed amount of uPAR on its cell surface. However, one could assume a varying surface density of uPAR due to external influence or active alteration by the cancer cells. Yang et al (2006), for example, have shown that subpopulations of colon cancer cells with an initially low cell surface uPAR number can spontaneously develop an oscillating cell surface uPAR density. In our general modelling framework it is possible to capture such a mechanism by adding an additional i-state variable describing the surface concentration of uPAR.

Intracellular reactions. In this work, we describe how to model surface-bound reactions in a structured-population approach. Such a structured approach is also suitable to describe intracellular reactions and the effect of the exchange of molecules between the cell's cytoplasm and the extracellular space or even the cell membrane. The corresponding changes in cell state will in many cases have an influence on the cell's behaviour. These processes can be expressed by making use of a structured cell volume density which is defined assuming a fixed volume for each cell. The latter is analogous to the structured cell surface density $s(t, x, y)$, as considered in this work, for which we assume a fixed cell surface area ε.

Higher order approximations in non-structured model. In the derivation of a non-structured model from the general structured model (18) it is necessary to approximate terms involving structured expressions with expressions that involve only non-structured variables. In Section 2.5, we use i-state mean values of all corresponding structured terms. Basically it is possible to consider more sophisticated, higher order approximations of these terms in order to incorporate the structural information in a more refined manner.

Structural flux and relation to age-structured models. Our general model (18a) as well as age-structured models are hyperbolic in the i-state/age variable. Accordingly, the prescription of boundary conditions on the i-state space has to be handled with care and is only possible at inflow boundary parts. The transport coefficient w.r.t. age in age-structured models is constant and uniform and thus the inflow boundary is *a priori* known and no "crossing of characteristics" is possible. In contrast to that, the transport coefficient in our structured model is given by the net binding rate, which depends on the i-state y and the free molecular volume concentrations $\mathbf{m}$. It is thus in general a nonuniform and nonlinear expression and hence changes in the i-state and with time. Thus, firstly, the inflow boundary, where the scalar product of the net binding rate and the unit outward normal vector is negative, may change with time and also a "crossing of characteristics" is possible. Further analytic investigations are required to give more insight into these issues and, more general, addressing rigorously the existence, uniqueness, and positivity of solutions of the proposed model.

A A Measure Theoretic Setting

A measure theoretical justification of the binding and unbinding rates introduced to define the structural flux given in (14) is as follows. Let $\mathfrak{B}(\mathcal{P})$ denote the Borel $\sigma-$algebra of the i-state space $\mathcal{P}$. In our model, given a density of molecular species $\mathbf{m}(t, x)$, the structural measure of their binding rate to the total cell density $C(t, x)$ is denoted by $\eta_{\mathbf{b}}(\cdot; \mathbf{m}) : \mathfrak{B}(\mathcal{P}) \to \mathbb{R}^p$ and is assumed to be absolutely continuous with respect to the Lebesgue measure on $\mathcal{P}$.

Then the induced Lebesgue-Radon-Nikodym density

$$\mathbf{b}(\cdot;\mathbf{m}) = \begin{pmatrix} b_1(\cdot;\mathbf{m}) \\ \vdots \\ b_p(\cdot;\mathbf{m}) \end{pmatrix} : \mathcal{P} \to \mathbb{R}^p \,. \tag{43}$$

is uniquely defined by

$$\eta_{\mathbf{b}}(W;\mathbf{m}) = \int_W \mathbf{b}(\gamma;\mathbf{m})\,\mathrm{d}\gamma\,, \quad \forall W \in \mathfrak{B}(\mathcal{P})\,, \tag{44}$$

(Halmos, 1978), and represents the binding rate of the molecular species $\mathbf{m}$ to the cell population density c.

Similarly, the structural measure of their unbinding rate of the bound molecular species $\mathbf{n}(t,x)$ is denoted by $\eta_{\mathbf{d}}$ and is again assumed to be absolutely continuous with respect to the Lebesgue measure on $\mathcal{P}$. Thus, this leads to an unbinding rate depending only on the i-state given by the Lebesgue-Radon-Nikodym density

$$\mathbf{d}(\cdot) = \begin{pmatrix} d_1(\cdot) \\ \vdots \\ d_p(\cdot) \end{pmatrix} : \mathcal{P} \to \mathbb{R}^p \tag{45}$$

is uniquely defined by

$$\eta_{\mathbf{d}}(W) = \int_W \mathbf{d}(\gamma)\,\mathrm{d}\gamma\,, \quad \forall W \in \mathfrak{B}(\mathcal{P})\,. \tag{46}$$

B The Source Term for Arbitrary Borel Sets $W \subset \mathcal{P}$

Let $W \subset \mathcal{P} \subset \mathbb{R}^p$ be an arbitrary Borel set and define $zW := \{zw : w \in W\}$ for $z \in \mathbb{R}$. If $z \neq 0$, we can also write $zW = \{\tilde{w} : \frac{1}{z}\tilde{w} \in W\}$. Assume that W, $2W$, and $\frac{1}{2}W$ are pairwise disjoint as shown in Fig. 1. Then, the source of cells in the structural region W that was obtained in (10) reads as

$$\int_W S(t,x,y)\,\mathrm{d}y = 2\int_{2W} \Phi(\tilde{y},\mathbf{u})c(t,x,\tilde{y})\,\mathrm{d}\tilde{y} - \int_W \Phi(y,\mathbf{u})c(t,x,y)\,\mathrm{d}y\,. \tag{47}$$

Note that we may have to invoke Convention 1 in the evaluation of the integral over $2W$. The purpose of this appendix is to show that Eq. (47) also holds for arbitrary Borel sets $W \subset \mathcal{P}$. We start with the following technical lemma.

Lemma 1 *Consider a set A such that $A \cap 2A = \emptyset$. Then it holds that $\frac{1}{2}A \cap A = \emptyset$ and, provided that A is also convex, $\frac{1}{2}A \cap 2A = \emptyset$.*

Proof Suppose there exists an $x \in \frac{1}{2}A \cap A$. Then $x \in A$ and it exists a $y \in A$ such that $x = \frac{1}{2}y$. This implies that $y = 2x$ is also an element of $2A$ and thus $y \in A \cap 2A$, a contradiction. Thus $\frac{1}{2}A \cap A = \emptyset$ must hold.

Now suppose there exists an $x \in \frac{1}{2}A \cap 2A$. Then there exist $y, z \in A$ such that $x = \frac{1}{2}z$ and $x = 2y$. Now observe that $x = \alpha y + (1-\alpha)z$ for $\alpha = \frac{2}{3} \in (0,1)$ and thus x can be written as a convex combination of y and z. Since A is convex, we also have $x \in A$. But then, $z = 2x \in A \cap 2A$, a contradiction. Thus $\frac{1}{2}A \cap 2A = \emptyset$ must hold. □

This enables us now to prove the following theorem.

Theorem 1 *Let W be an arbitrary convex and compact subset of $\mathcal{P}$. Then Eq.* (47) *holds.*

Proof Since $W \subset \mathcal{P}$ is an arbitrary convex and compact set, the sets W, $2W$, and $\frac{1}{2}W$ might not be pairwise disjoint. Since W is compact, we have that the Lebesgue measure $\lambda(W) < \infty$. Furthermore, it holds that $\lambda(zW) = z^p\lambda(W)$ for all $z \in \mathbb{R}$. We define the sequence of sets

$$W_k := \bigcap_{i=0}^{k} 2^{-i}W, \quad k = 0, 1, 2, \dots .$$

These sets are, as intersection of convex sets, convex and have the following properties

$$W_0 = W\,, \quad W_j \subseteq W_i \text{ for all } j \geq i\,, \quad \text{and} \quad \lambda(W_k) \leq 2^{-pk}\lambda(W)\,.$$

Note that if $0 \notin W$ then there exists a finite K such that $W_k = \emptyset$ for all $k \geq K$, otherwise, if $0 \in W$ then $0 \in W_k$ for all k and $\lim_{k\to\infty} W_k = \{0\}$. Therefore, combining both cases, define $W_\infty := \{0\} \cap W$; clearly $\lambda(W_\infty) = 0$. Thus we can write

$$W = W_0 = W_0 \setminus W_1 \cup W_1 = \ldots = \left(\dot{\bigcup_{i=0}^{k}} W_i \setminus W_{i+1}\right) \cup W_{k+1} = \left(\dot{\bigcup_{i=0}^{\infty}} A_i\right) \cup W_\infty\,,$$

where $A_k := W_k \setminus W_{k+1}$ for $k = 0, 1, \dots$. From the definition of the sets W_k we can also deduce the following relation

$$2W_k = 2W \cap W_{k-1} \text{ for } k = 1, 2, \dots .$$

Now, for all $k = 0, 1, 2, \dots$ we obtain

$$\begin{aligned} A_k \cap 2A_k &= (W_k \setminus W_{k+1}) \cap (2W_k) \setminus (2W_{k+1}) \\ &= (W_k \setminus W_{k+1}) \cap (2W_k) \setminus (2W \cap W_k) \\ &= (W_k \setminus W_{k+1}) \cap \Big[\underbrace{((2W_k) \setminus (2W))}_{=\emptyset} \cup ((2W_k) \setminus W_k)\Big] \\ &= (W_k \setminus W_{k+1}) \cap ((2W_k) \setminus W_k) \\ &= \emptyset\,. \end{aligned}$$

Following the first part of Lemma 1 it now also follows that $\frac{1}{2}A_k \cap A_k = \emptyset$ for $k = 0, 1, 2, \dots$. The second part of Lemma 1 is not applicable here since A_k is in general not convex. However, note that the derivation above also shows that

$$2A_k = (2W_k) \setminus W_k \text{ for } k = 0, 1, 2, \dots .$$

Using that relation, once directly and once multiplied by $\frac{1}{4}$, we now obtain, for all $k = 0, 1, 2, \dots$,

$$\frac{1}{2}A_k \cap 2A_k = \left(\left(\frac{1}{2}W_k\right) \setminus \left(\frac{1}{4}W_k\right)\right) \cap \left((2W_k) \setminus W_k\right).$$

Now assume that there exists an $x \in \frac{1}{2}A_k \cap 2A_k$. Then necessarily, $x \in \frac{1}{2}W_k$ and $x \in 2W_k$. As in the proof of the second part of Lemma 1 it follows, thanks to the convexity of W_k, that also $x \in W_k$. However, then $x \notin (2W_k) \setminus W_k$ and thus $x \notin \frac{1}{2}A_k \cap 2A_k$, a contradiction. Thus it also holds that $\frac{1}{2}A_k \cap 2A_k = \emptyset$.

In summary, it holds that, for each $k = 0, 1, 2, \dots$, the sets A_k, $2A_k$, and $\frac{1}{2}A_k$ are pairwise disjoint and hence Eq. (47) holds with W replaced by A_k.

Now we can conclude for our arbitrary convex and compact set $W \subset \mathcal{P}$, that

$$\begin{aligned}
\int_W S(t,x,y)\,\mathrm{d}y &= \int_{\bigcup_{i=0}^{\infty} A_i} S(t,x,y)\,\mathrm{d}y = \sum_{i=0}^{\infty} \int_{A_i} S(t,x,y)\,\mathrm{d}y \\
&\overset{(47)}{=} \sum_{i=0}^{\infty} \left[2 \int_{2A_i} \Phi(\tilde{y},\mathbf{u}) c(t,x,\tilde{y})\,\mathrm{d}\tilde{y} - \int_{A_i} \Phi(y,\mathbf{u}) c(t,x,y)\,\mathrm{d}y \right] \\
&= 2 \int_{\bigcup_{i=0}^{\infty} 2A_i} \Phi(\tilde{y},\mathbf{u}) c(t,x,\tilde{y})\,\mathrm{d}\tilde{y} - \int_{\bigcup_{i=0}^{\infty} A_i} \Phi(y,\mathbf{u}) c(t,x,y)\,\mathrm{d}y \\
&= 2 \int_{2W} \Phi(\tilde{y},\mathbf{u}) c(t,x,\tilde{y})\,\mathrm{d}\tilde{y} - \int_{W} \Phi(y,\mathbf{u}) c(t,x,y)\,\mathrm{d}y\,.
\end{aligned}$$

□

Since we have shown that Eq. (47) holds for arbitrary convex and compact subsets of $\mathcal{P}$, it in particular also holds for all rectangles, which are a family of generators of the Borelian σ-algebra on $\mathcal{P}$ (Halmos, 1978). Hence it holds for all Borel subsets of $\mathcal{P}$.

C Non-Dimensionalisation and Parameter Tables

Based on a typical cancer cell volume of $1.5 \cdot 10^{-8}\mathrm{cm}^3$, see Anderson (2005) and references cited there, we set

$$\vartheta_c = 1.5 \cdot 10^{-8}\mathrm{cm}^3/\mathrm{cell}$$

and define the scaling parameter $c_* = 1/\vartheta_c = 6.7 \cdot 10^7 \mathrm{cells/cm}^3$ as the inverse of ϑ_c, i.e., taken as the maximum cell density such that no overcrowding occurs. Assuming that a cell is approximately a sphere, we obtain a surface area of $\varepsilon = 2.94 \cdot 10^{-5}\mathrm{cm}^2/\mathrm{cell}$. In Lodish et al (2007), the amount of surface receptors is given by a range from 1,000 to 50,000 molecules per cell. We take the upper limit which is translated to $50,000$ molecules/cell $= 8.3 \cdot 10^{-14}$ µmol/cell and gives a reference surface density of

$$y_* = \frac{8.3 \cdot 10^{-14}\mu\mathrm{mol/cell}}{2.94 \cdot 10^{-5}\mathrm{cm}^2/\mathrm{cell}} = 2.82 \cdot 10^{-9}\mu\mathrm{mol/cm}^2.$$

In Abreu et al (2010) it is stated that the collagen density in engineered provisional scaffolds should be between 2 and 4 $\mathrm{mg/cm}^3$ for *in vivo* delivery. We take the upper limit as scaling parameter v_* for the ECM density. Assuming that ECM at this density fills up all available physical space, we obtain $1 = \rho(0, v_*) = \vartheta_v v_*$ and thus

$$\vartheta_v := \frac{1}{v_*}\,.$$

Note that with these these scalings we have already for the volume fraction of occupied space, cf. (5),

$$\rho(C,v) = \vartheta_c C + \vartheta_v v = \vartheta_c c_* \tilde{C} + \vartheta_v v_* \tilde{v} = \tilde{\vartheta}_c \tilde{C} + \tilde{\vartheta}_v \tilde{v} = \tilde{C} + \tilde{v} = \tilde{\rho}(\tilde{C},\tilde{v})\,.$$

The scaling parameters $\tau = 10^4$s and $L = 0.1$cm are chosen as in Gerisch and Chaplain (2008) and Domschke et al (2014) and, as in loc. cit., the value of the scaling parameter m_* remains unspecified. Table 1 shows the model parameters with units and their non-dimensionalised counterparts, and intermediate quantities of these can be found in Table 2.

p	unit	$\tilde{p}$	conditions
ε	$\mathrm{cm}^2/\mathrm{cell}$	$\frac{c_* y_*}{m_*}\varepsilon$	$\varepsilon > 0$
ϑ_c	$\mathrm{cm}^3/\mathrm{cell}$	$c_*\vartheta_c$	$\vartheta_c > 0$
ϑ_v	$\mathrm{cm}^3/\mathrm{mg}$	$v_*\vartheta_v$	$\vartheta_v > 0$
D_c	cm^2/s	$\frac{\tau}{L^2}D_c$	$D_c > 0$
χ_k	$(\mathrm{cm}^2/\mathrm{s})/\mathrm{nM}$	$\frac{\tau}{L^2}m_*\chi_k$	$\chi_k \geq 0$, $k = 1, \ldots, q$
χ_v	$(\mathrm{cm}^2/\mathrm{s})/(\mathrm{mg}/\mathrm{cm}^3)$	$\frac{\tau}{L^2}v_*\chi_v$	$\chi_v \geq 0$
$\boldsymbol{\delta}_v$	$1/(\mathrm{nM\,s})$	$\tau m_* \boldsymbol{\delta}_v$	$\boldsymbol{\delta}_v \geq 0$
$\mathbf{D_m}$	cm^2/s	$\frac{\tau}{L^2}\mathbf{D_m}$	$\mathbf{D_m} > 0$
$\boldsymbol{\delta_m}$	$1/\mathrm{s}$	$\tau\boldsymbol{\delta_m}$	$\boldsymbol{\delta_m} \geq 0$

Table 1: Parameters p of the general model (18) with their unit and their non-dimensionalised counterparts $\tilde{p}$.

p	unit	$\tilde{p}$	references/notes
$\rho(C, v)$	—	ρ	volume fraction of occupied space
$\Phi(y, \mathbf{u})$	$1/\mathrm{s}$	$\tau\Phi$	i-state-dependent cell proliferation rate
$\mathbf{b}(y, \mathbf{m})$	$(\mu\mathrm{mol}/\mathrm{cm}^2)/\mathrm{s}$	$\frac{\tau}{y_*}\mathbf{b}$	vector of binding rates of molecular species, $\mathbf{b} \geq 0$,
$\mathbf{d}(y)$	$(\mu\mathrm{mol}/\mathrm{cm}^2)/\mathrm{s}$	$\frac{\tau}{y_*}\mathbf{d}$	vector of unbinding/detaching rates of molecular species, $\mathbf{d} \geq 0$,
$\psi_v(t, \mathbf{u})$	$(\mathrm{mg}/\mathrm{cm}^3)/\mathrm{s}$	$\frac{\tau}{v_*}\psi$	ECM remodelling law, $\psi_v \geq 0$ if $v = 0$
$\boldsymbol{\psi}_\mathbf{m}(\mathbf{u}, \mathbf{r})$	$\mathrm{nM/s}$	$\frac{\tau}{m_*}\boldsymbol{\psi}_\mathbf{m}$	vector of production terms for molecular species, $\boldsymbol{\psi}_\mathbf{m} \geq \mathbf{0}$

Table 2: Intermediate model quantities p of the general model (18) with their unit and their non-dimensionalised counterparts $\tilde{p}$. The latter have to be read, for instance, as follows $\tilde{\mathbf{b}}(\tilde{y}, \tilde{\mathbf{m}}) = \frac{\tau}{y_*}\mathbf{b}(y, \mathbf{m})$.

Acknowledgements PD was supported by the Northern Research Partnership PECRE scheme and the Deutsche Forschungsgemeinschaft under the grant DO 1825/1-1. DT and AG would like to acknowledge Northern Research Partnership PECRE scheme. DT and MAJC gratefully acknowledge the support of the ERC Advanced Investigator Grant 227619, "M5CGS - From Mutations to Metastases: Multiscale Mathematical Modelling of Cancer Growth and Spread". The authors PD, DT, AG, and MAJC would like to thank the Isaac Newton Institute for Mathematical Sciences for its hospitality during the programme "*Coupling Geometric PDEs with Physics for Cell Morphology, Motility and Pattern Formation*" supported by EPSRC Grant Number EP/K032208/1.

References

Abia L, Angulo O, López-Marcos J, López-Marcos M (2009) Numerical schemes for a size-structured cell population model with equal fission. Math Comput Model 50(5–6):653 – 664, DOI 10.1016/j.mcm.2009.05.023

Abreu EL, Palmer MP, Murray MM (2010) Collagen density significantly affects the functional properties of an engineered provisional scaffold. J Biomed Mater Res Part A 93A(1):150–157, DOI 10.1002/jbm.a.32508

Ainseba B, Anita S (2001) Local exact controllability of the age-dependent population dynamics with diffusion. Abstr Appl Anal 6(6):357–368, DOI 10.1155/S108533750100063X

Ainseba B, Langlais M (2000) On a population dynamics control problem with age dependence and spatial structure. J Math Anal Appl 248(2):455–474, DOI 10.1006/jmaa.2000.6921

Al-Omari J, Gourley S (2002) Monotone travelling fronts in an age-structured reaction-diffusion model of a single species. J Math Biol 45(4):294–312, DOI 10.1007/s002850200159

Allen EJ (2009) Derivation of stochastic partial differential equations for size- and age-structured populations. J Biol Dyn 3(1):73–86, DOI 10.1080/17513750802162754

Andasari V, Gerisch A, Lolas G, South AP, Chaplain MA (2011) Mathematical modeling of cancer cell invasion of tissue: biological insight from mathematical analysis and computational simulation. J Math Biol 63(1):141–171, DOI 10.1007/s00285-010-0369-1

Anderson A, Chaplain M (1998) Continuous and discrete mathematical models of tumor-induced angiogenesis. Bull Math Biol 60(5):857–899, DOI 10.1006/bulm.1998.0042

Anderson ARA (2005) A hybrid mathematical model of solid tumour invasion: the importance of cell adhesion. IMA J Math Med Biol 22(2):163–186, DOI 10.1093/imammb/dqi005

Anderson ARA, Chaplain MAJ, Newman EL, Steele RJC, Thompson AM (2000) Mathematical modelling of tumour invasion and metastasis. J Theor Med 2(2):129–154, DOI 10.1080/10273660008833042

Andreasen PA, Kjøller L, Christensen L, Duffy MJ (1997) The urokinase-type plasminogen activator system in cancer metastasis: A review. Int J Cancer 72(1):1–22, DOI 10.1002/(SICI)1097-0215(19970703)72:1⟨1::AID-IJC1⟩3.0.CO;2-Z

Andreasen PA, Egelund R, Petersen HH (2000) The plasminogen activation system in tumor growth, invasion, and metastasis. Cell Mol Life Sci 57(1):25–40, DOI 10.1007/s000180050497

Angulo O, López-Marcos J, Bees M (2012) Mass structured systems with boundary delay: Oscillations and the effect of selective predation. J Nonlinear Sci 22(6):961–984, DOI 10.1007/s00332-012-9133-6

Armstrong NJ, Painter KJ, Sherratt JA (2006) A continuum approach to modelling cell–cell adhesion. J Theor Biol 243(1):98–113, DOI 10.1016/j.jtbi.2006.05.030

Ayati B (2000) A variable time step method for an age-dependent population model with nonlinear diffusion. SIAM J Num Anal 37(5):1571–1589, DOI 10.1137/S003614299733010X

Ayati B, Dupont T (2002) Galerkin methods in age and space for a population model with nonlinear diffusion. SIAM J Num Anal 40(3):1064–1076, DOI 10.1137/S0036142900379679

Ayati B, Webb G, Anderson A (2006) Computational methods and results for structured multiscale models of tumor invasion. Multiscale Model Simul 5(1):1–20, DOI 10.1137/050629215

Ayati BP (2006) A structured-population model of proteus mirabilis swarm-colony development. J Math Biol 52(1):93–114, DOI 10.1007/s00285-005-0345-3

Bafetti L, Young T, Itoh Y, Stack S (1998) Intact vitronectin induces matrix metalloproteinase-2 and tissue inhibitor of metalloproteinase-2 expression and enhanced cellular invasion by melanoma cells. J Biol Chem 273:143–149

Basse B, Ubezio P (2007) A generalised age- and phase-structured model of human tumour cell populations both unperturbed and exposed to a range of cancer therapies. Bull Math Biol 69(5):1673–1690, DOI 10.1007/s11538-006-9185-6

Basse B, Baguley BC, Marshall ES, Joseph WR, van Brunt B, Wake G, Wall DJN (2003) A mathematical model for analysis of the cell cycle in cell lines derived from human tumors. J Math Biol 47(4):295–312, DOI 10.1007/s00285-003-0203-0

Basse B, Baguley BC, Marshall ES, Joseph WR, van Brunt B, Wake G, Wall DJ (2004) Modelling cell death in human tumour cell lines exposed to the anticancer drug paclitaxel. J Math Biol 49(4):329–357, DOI 10.1007/s00285-003-0254-2

Basse B, Baguley B, Marshall E, Wake G, Wall D (2005) Modelling the flow of cytometric data obtained from unperturbed human tumour cell lines: Parameter fitting and comparison. Bull Math Biol 67(4):815–830, DOI 10.1016/j.bulm.2004.10.003

Bélair J, Mackey MC, Mahaffy JM (1995) Age-structured and two-delay models for erythropoiesis. Math Biosci 128(1–2):317–346, DOI 10.1016/0025-5564(94)00078-E

Bernard S, Pujo-Menjouet L, Mackey MC (2003) Analysis of cell kinetics using a cell division marker: Mathematical modeling of experimental data. Biophys J 84(5):3414–3424, DOI 10.1016/S0006-3495(03)70063-0

Billy F, Clairambaultt J, Fercoq O, Gaubertt S, Lepoutre T, Ouillon T, Saito S (2014) Synchronisation and control of proliferation in cycling cell population models with age structure. Math Comput Simul 96:66–94, DOI 10.1016/j.matcom.2012.03.005

Busenberg S, Iannelli M (1983) A class of nonlinear diffusion problems in age-dependent population dynamics. Nonlinear Anal Theor Meth Appl 7(5):501–529, DOI 10.1016/0362-546X(83)90041-X

Byrne HM, Preziosi L (2004) Modelling solid tumour growth using the theory of mixtures. Math Med Biol 20:341–366, DOI 10.1093/imammb/20.4.341

Calsina À, Saldaña J (1995) A model of physiologically structured population dynamics with a nonlinear individual growth rate. J Math Biol 33(4):335–364, DOI 10.1007/BF00176377

de Camino-Beck T, Lewis M (2009) Invasion with stage-structured coupled map lattices: Application to the spread of scentless chamomile. Ecol Model 220(23):3394–3403, DOI 10.1016/j.ecolmodel.2009.09.003

Chaplain M, Lolas G (2005) Mathematical modelling of cancer cell invasion of tissue: the role of the urokinase plasminogen activation system. Math Models Methods Appl Sci 15(11):1685–1734, DOI 10.1142/S0218202505000947

Chaplain MAJ, Lolas G (2006) Mathematical modelling of cancer invasion of tissue: Dynamic heterogeneity. Netw Hetero Media 1(3):399–439, DOI 10.3934/nhm.2006.1.399

Chapman SJ, Plank MJ, James A, Basse B (2007) A nonlinear model of age and size-structured populations with applications to cell cycles. ANZIAM J 49:151–169, DOI 10.1017/S144618110001275X

Cubellis MV, Wun TC, Blasi F (1990) Receptor-mediated internalization and degradation of urokinase is caused by its specific inhibitor PAI-1. EMBO J 9(4):1079–1085

Cushing JM (1998) An Introduction to Structured Population Dynamics, CBMS-NSF Regional Conference Series in Applied Mathematics, vol 71. SIAM, DOI 10.1137/1.9781611970005.ch2

Cusulin C, Iannelli M, Marinoschi G (2005) Age-structured diffusion in a multi-layer environment. Nonlinear Anal Real World Appl 6(1):207–223, DOI 10.1016/j.nonrwa.2004.08.006

Daukste L, Basse B, Baguley B, Wall D (2012) Mathematical determination of cell population doubling times for multiple cell lines. Bull Math Biol 74(10):2510–2534, DOI 10.1007/s11538-012-9764-7

Deakin N, Chaplain MAJ (2013) Mathematical modelling of cancer invasion: The role of membrane-bound matrix metalloproteinases. Frontiers in Oncology 3(70), DOI 10.3389/fonc.2013.00070

Deisboeck TS, Wang Z, Macklin P, Cristini V (2011) Multiscale cancer modeling. Annu Rev Biomed Eng 13:127–155, DOI 10.1146/annurev-bioeng-071910-124729

Delgado M, Molina-Becerra M, Suárez A (2006) A nonlinear age-dependent model with spatial diffusion. J Math Anal Appl 313(1):366–380, DOI 10.1016/j.jmaa.2005.09.042

Deng Q, Hallam TG (2006) An age structured population model in a spatially heterogeneous environment: Existence and uniqueness theory. Nonlinear Anal Theor Meth Appl 65(2):379–394, DOI 10.1016/j.na.2005.06.019

Di Blasio G (1979) Non-linear age-dependent population diffusion. J Math Biol 8(3):265–284, DOI 10.1007/BF00276312

Diekmann O, Metz J (1994) On the reciprocal relationship between life histories and population dynamics. In: Levin S (ed) Frontiers in Mathematical Biology, Lecture Notes in Biomathematics, vol 100, Springer Berlin Heidelberg, pp 263–279, DOI 10.1007/978-3-642-50124-1_16

Diekmann O, Heijmans H, Thieme H (1984) On the stability of the cell size distribution. J Math Biol 19(2):227–248, DOI 10.1007/BF00277748

Diekmann O, Gyllenberg M, Metz JAJ, Thieme H (1992) The 'Cumulative' Formulation of (Physiologically) Structured Population Models. CWI

Domschke P, Trucu D, Gerisch A, Chaplain MAJ (2014) Mathematical modelling of cancer invasion: Implications of cell adhesion variability for tumour infiltrative growth patterns. J Theor Biol 361:41–60, DOI 10.1016/j.jtbi.2014.07.010

Duffy MJ (2004) The urokinase plasminogen activator system: Role in malignancy. Curr Pharm Des 10(1):39–49, DOI 10.2174/1381612043453559

Engwer C, Hillen T, Knappitsch M, Surulescu C (2015) Glioma follow white matter tracts: a multiscale dti-based model. J Math Biol 71(3):551–582, DOI 10.1007/s00285-014-0822-7

Erban R, Othmer HG (2005) From signal transduction to spatial pattern formation in e. coli: A paradigm for multiscale modeling in biology. Multiscale Model Simul 3(2):362–394, DOI 10.1137/040603565

Fitzgibbon W, Parrott M, Webb G (1995) Diffusion epidemic models with incubation and crisscross dynamics. Math Biosci 128(1–2):131–155, DOI 10.1016/0025-5564(94)00070-G

von Foerster H (1959) Some remarks on changing populations. In: Stohlman JF (ed) The Kinetics of Cellular Proliferation, Grune and Stratton, New York, pp 382–407

Foley C, Mackey M (2009) Dynamic hematological disease: a review. J Math Biol 58(1-2):285–322, DOI 10.1007/s00285-008-0165-3

Förste J (1978) Diekmann, O. / Temme, N. M. (Hrsg.), Nonlinear Diffusion Problems. Amsterdam. Mathematisch Centrum. ZAMM 58(12):583–584, DOI 10.1002/zamm.19780581223

Gabriel P, Garbett SP, Quaranta V, Tyson DR, Webb GF (2012) The contribution of age structure to cell population responses to targeted therapeutics. J Theor Biol 311(0):19–27, DOI 10.1016/j.jtbi.2012.07.001

Garroni MG, Langlais M (1982) Age-dependent population diffusion with external constraint. J Math Biol 14(1):77–94, DOI 10.1007/BF02154754

Gatenby RA, Gawlinski ET (1996) A reaction-diffusion model of cancer invasion. Cancer Res 56:5745–5753

Gerisch A, Chaplain M (2008) Mathematical modelling of cancer cell invasion of tissue: Local and non-local models and the effect of adhesion. J Theor Biol 250(4):684–704, DOI 10.1016/j.jtbi.2007.10.026

Gurtin M, MacCamy R (1981) Diffusion models for age-structured populations. Math Biosci 54(1–2):49–59, DOI 10.1016/0025-5564(81)90075-4

Gwiazda P, Marciniak-Czochra A (2010) Structured population equations in metric spaces. J Hyperbol Diff Eq 07(04):733–773, DOI 10.1142/S021989161000227X

Gyllenberg M (1982) Nonlinear age-dependent population dynamics in continuously propagated bacterial cultures. Math Biosci 62(1):45–74, DOI 10.1016/0025-5564(82)90062-1

Gyllenberg M (1983) Stability of a nonlinear age-dependent population model containing a control variable. SIAM J Appl Math 43(6):1418–1438, URL `http://www.jstor.org/stable/2101185`

Gyllenberg M (1986) The size and scar distributions of the yeast saccharomyces cerevisiae. J Math Biol 24(1):81–101, DOI 10.1007/BF00275722

Gyllenberg M, Hanski I (1997) Habitat deterioration, habitat destruction, and metapopulation persistence in a heterogenous landscape. Theor Popul Biol 52(3):198–215, DOI 10.1006/tpbi.1997.1333

Gyllenberg M, Webb G (1987) Age-size structure in populations with quiescence. Math Biosci 86(1):67–95, DOI 10.1016/0025-5564(87)90064-2

Gyllenberg M, Webb G (1990) A nonlinear structured population model of tumor growth with quiescence. J Math Biol 28(6):671–694, DOI 10.1007/BF00160231

Gyllenberg M, Hanski I, Lindström T (1997) Continuous versus discrete single species population models with adjustable reproductive strategies. Bull Math Biol 59(4):679–705, DOI 10.1007/BF02458425

Gyllenberg M, Osipov A, Päivärinta L (2002) The inverse problem of linear age-structured population dynamics. J Evol Eq 2(2):223–239, DOI 10.1007/s00028-002-8087-9
Halmos PR (1978) Measure Theory, 2nd edn. Springer
Huang C (1994) An age-dependent population model with nonlinear diffusion in $\mathbf{R}^n$. Quart Appl Math 52:377–398
Huyer W (1994) A size-structured population-model with dispersion. J Math Anal Appl 181(3):716–754, DOI 10.1006/jmaa.1994.1054
Kelkel J, Surulescu C (2012) A multiscale approach to cell migration in tissue networks. Math Models Methods Appl Sci 22(03):1150,017 [25 pages], DOI 10.1142/S0218202511500175
Kunisch K, Schappacher W, Webb GF (1985) Nonlinear age-dependent population dynamics with random diffusion. Comput Math Applic 11(1–3):155–173, DOI 10.1016/0898-1221(85)90144-0
Langlais M (1988) Large time behavior in a nonlinear age-dependent population dynamics problem with spatial diffusion. J Math Biol 26(3):319–346, DOI 10.1007/BF00277394
Langlais M, Milner FA (2003) Existence and uniqueness of solutions for a diffusion model of host–parasite dynamics. J Math Anal Appl 279(2):463–474, DOI 10.1016/S0022-247X(03)00020-9
Laurençot P, Walker C (2008) An age and spatially structured population model for proteus mirabilis swarm-colony development. Math Model Nat Phenom 3(7):49–77, DOI 10.1051/mmnp:2008041
Lewis M, Nelson W, Xu C (2010) A structured threshold model for mountain pine beetle outbreak. Bull Math Biol 72(3):565–589, DOI 10.1007/s11538-009-9461-3
Lodish H, Berk A, Kaiser CA, Krieger M, Scott MP, Bretscher A, Ploegh H, Matsudaira P (2007) Molecular Cell Biology, 6th edn. W.H.Freeman
MacCamy R (1981) A population model with nonlinear diffusion. J Diff Eq 39(1):52–72, DOI 10.1016/0022-0396(81)90083-8
Mackey M, Glass L (1977) Oscillation and chaos in physiological control systems. Science 197(4300):287–289, DOI 10.1126/science.267326
Macklin P, McDougall SR, Anderson ARA, Chaplain MAJ, Cristini V, Lowengrub J (2009) Multiscale modelling and nonlinear simulation of vascular tumour growth. J Math Biol 58:765–798, DOI 10.1007/s00285-008-0216-9
Mahaffy JM, Bélair J, Mackey MC (1998) Hematopoietic model with moving boundary condition and state dependent delay: Applications in erythropoiesis. J Theor Biol 190(2):135–146, DOI 10.1006/jtbi.1997.0537
Marciniak-Czochra A, Ptashnyk M (2008) Derivation of a macroscopic receptor-based model using homogenization techniques. SIAM J Math Anal 40(1):215–237, DOI 10.1137/050645269
Matter SF, Hanski I, Gyllenberg M (2002) A test of the metapopulation model of the species–area relationship. J Biogeo 29(8):977–983, DOI 10.1046/j.1365-2699.2002.00748.x
Mercker M, Marciniak-Czochra A, Richter T, Hartmann D (2013) Modeling and computing of deformation dynamics of inhomogeneous biological surfaces. SIAM J Appl Math 73(5):1768–1792, DOI 10.1137/120885553
Metz JAJ, Diekmann O (1986) The Dynamics of Physiologically Structured Populations, Lecture Notes in Biomathematics, vol 68. Springer-Verlag
Othmer HG, Xue C (2013) Dispersal, Individual Movement and Spatial Ecology: A Mathematical Perspective, Springer Berlin Heidelberg, Berlin, Heidelberg, chap The Mathematical Analysis of Biological Aggregation and Dispersal: Progress, Problems and Perspectives, pp 79–127. DOI 10.1007/978-3-642-35497-7_4
Othmer HG, Dunbar SR, Alt W (1988) Models of dispersal in biological systems. J Math Biol 26(3):263–298, DOI 10.1007/BF00277392
Parsons SL, Watson SA, Brown PD, Collins HM, Steele RJ (1997) Matrix metalloproteinases. Brit J Surg 84(2):160–166, DOI 10.1046/j.1365-2168.1997.02719.x
Pepper MS (2001) Role of the matrix metalloproteinase and plasminogen activator-plasmin systems in angiogenesis. Arterioscl Throm Vas 21(7):1104–1117, DOI 10.1161/hq0701.093685
Perthame B (2007) Transport Equations in Biology. Frontiers in Mathematics, Birkhäuser
Ramis-Conde I, Drasdo D, Anderson ARA, Chaplain MAJ (2008) Modeling the influence of the e-cadherin-β-catenin pathway in cancer cell invasion: A multiscale approach. Biophys

J 95(1):155–165, DOI 10.1529/biophysj.107.114678
Rhandi A (1998) Positivity and stability for a population equation with diffusion on l^1. Positivity 2(2):101–113, DOI 10.1023/A:1009721915101
Rhandi A, Schnaubelt R (1999) Asymptotic behaviour of a non-autonomous population equation with diffusion in L^1. Discr Cont Dyn Sys Series A 5(3):663–683, DOI 10.3934/dcds.1999.5.663
Roeder I, Herberg M, Horn M (2009) An "age" structured model of hematopoietic stem cell organization with application to chronic myeloid leukemia. Bull Math Biol 71(3):602–626, DOI 10.1007/s11538-008-9373-7
de Roos AM (1997) A gentle introduction to physiologically structured population models. In: Tuljapurkar S, Caswell H (eds) Structured-Population Models in Marine, Terrestrial, and Freshwater Systems, Population and Community Biology Series, vol 18, Springer US, pp 119–204, DOI 10.1007/978-1-4615-5973-3_5
Rowe R, Weiss S (2009) Navigating ecm barriers at the invasive front: the cancer cell-stroma interface. Annu Rev Cell Dev Biol 25:567–595, DOI 10.1146/annurev.cellbio.24.110707.175315
Sabeh F, Ota I, Holmbeck K, Birkedal-Hansen H, Soloway P, Balbin M, Lopez-Otin C, Shapiro S, Inada M, Krane S, Allen E, Chung D, Weiss S (2004) Tumor cell traffic through the extracellular matrix is controlled by the membrane-anchored collagenase mt1-mmp. J Cell Biol 167(4):769–781, DOI 10.1083/jcb.200408028
Sabeh F, Shimizu-Hirota R, Weiss S (2009) Protease-dependent versus -independent cancer cell invasion programs: three-dimensional amoeboid movement revisited. J Cell Biol 185(1):11–19, DOI 10.1083/jcb.200807195
Sinko JW, Streifer W (1967) A new model for age-size structure of a population. Ecology 48(6):910–918, DOI 10.2307/1934533
Skellam JG (1951) Random dispersal in theoretical populations. Biometrika 38(1/2):196–218, DOI 10.2307/2332328
So JWH, Wu J, Zou X (2001) A reaction-diffusion model for a single species with age structure. i travelling wavefronts on unbounded domains. Proc Roy Soc Lond A 457(2012):1841–1853, DOI 10.1098/rspa.2001.0789
Trucco E (1965a) Mathematical models for cellular systems the von foerster equation. part i. Bull Math Biophys 27(3):285–304, DOI 10.1007/BF02478406
Trucco E (1965b) Mathematical models for cellular systems. the von foerster equation. part ii. Bull Math Biophys 27(4):449–471, DOI 10.1007/BF02476849
Trucu D, Lin P, Chaplain MAJ, Wang Y (2013) A multiscale moving boundary model arising in cancer invasion. Multiscale Model Sim 11(1):309–335, DOI 10.1137/110839011
Tucker SL, Zimmerman SO (1988) A nonlinear model of population dynamics containing an arbitrary number of continuous structure variables. SIAM J Appl Math 48(3):pp. 549–591, URL `http://www.jstor.org/stable/2101595`
Ulisse S, Baldini E, Sorrenti S, D'Armiento M (2009) The urokinase plasminogen activator system: A target for anti-cancer therapy. Curr Cancer Drug Targets 9(1):32–71, DOI 10.2174/156800909787314002
Walker C (2007) Global well-posedness of a haptotaxis model with spatial and age structure. Diff Int Eq 20(9):1053–1074, URL `http://projecteuclid.org/euclid.die/1356039311`
Walker C (2008) Global existence for an age and spatially structured haptotaxis model with nonlinear age-boundary conditions. Europ J Appl Math 19:113–147, DOI 10.1017/S095679250800733X
Walker C (2009) Positive equilibrium solutions for age- and spatially-structured population models. SIAM J Math Anal 41(4):1366–1387, DOI 10.1137/090750044
Webb G (2008) Population models structured by age, size, and spatial position. In: Magal P, Ruan S (eds) Structured Population Models in Biology and Epidemiology, Lecture Notes in Mathematics, vol 1936, Springer Berlin Heidelberg, pp 1–49, DOI 10.1007/978-3-540-78273-5_1
Webb GF (1985) Theory of Nonlinear Age-dependent Population Dynamics, Pure and Applied Mathematics, vol 89. Marcel Dekker, New York
Xue C (2015) Macroscopic equations for bacterial chemotaxis: integration of detailed biochemistry of cell signaling. J Math Biol 70(1):1–44, DOI 10.1007/s00285-013-0748-5

Xue C, Othmer HG, Erban R (2009) From individual to collective behavior of unicellular organisms: Recent results and open problems. AIP Conference Proceedings 1167(1):3–14, DOI 10.1063/1.3246413

Xue C, Hwang HJ, Painter KJ, Erban R (2011) Travelling waves in hyperbolic chemotaxis equations. Bull Math Biol 73(8):1695–1733, DOI 10.1007/s11538-010-9586-4

Yang L, Avila H, Wang H, Trevino J, Gallick GE, Kitadai Y, Sasaki T, Boyd DD (2006) Plasticity in urokinase-type plasminogen activator receptor (upar) display in colon cancer yields metastable subpopulations oscillating in cell surface upar density – implications in tumor progression. Cancer Res 66(16):7957–7967, DOI 10.1158/0008-5472.CAN-05-3208